

Article

Supramolecular Diversity of Oxabicyclo[2.2.2]octenes Formed between Substituted 2*H*-Pyran-2-ones and Vinyl-Moiety-Containing Dienophiles

Krištof Kranjc, Amadej Juranovič, Marijan Kočevar and Franc Perdih * 

Faculty of Chemistry and Chemical Technology, University of Ljubljana, Večna pot 113, SI-1000 Ljubljana, Slovenia; kristof.kranjc@fkkt.uni-lj.si (K.K.); amadej.juranovic@fkkt.uni-lj.si (A.J.); marijan.kocevar@fkkt.uni-lj.si (M.K.)

* Correspondence: franc.perdih@fkkt.uni-lj.si; Tel.: +386-1-479-8527

Received: 8 October 2020; Accepted: 16 October 2020; Published: 17 October 2020



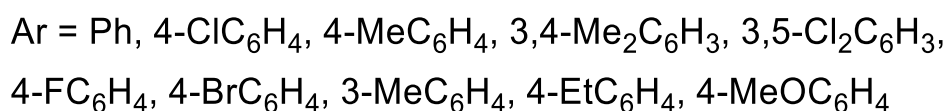
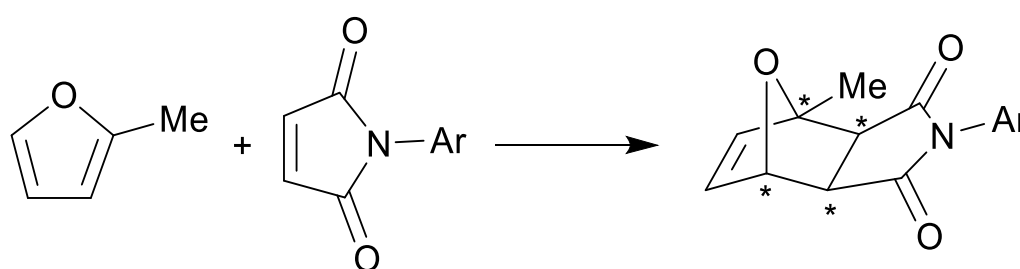
Abstract: In Diels–Alder reactions, 2*H*-pyran-2-ones as dienes can yield a large variety of cycloadducts with up to four contiguous carbon stereogenic centers. Some of the potentially most useful, however difficult to prepare due to their low thermal stability, are the primary CO₂-containing oxabicyclo[2.2.2]octenes, which could be formed as eight distinctive isomers (two sets of regioisomers, each of these composed of four different stereoisomers). A high-pressure synthesis of such products was recently described in a few cases where vinyl-moiety-containing dienophiles were used as synthetic equivalents of acetylene. However, structures of the primary products have been so far only rarely investigated in detail. Herein, we present seven novel single-crystal X-ray diffraction structures of such cycloadducts of both stereoisomeric forms, i.e., *endo* and *exo*. Additionally, we present a single-crystal structure of a rare case of a cyclohexadiene system stable at room temperature, obtained as a secondary product upon the retro-hetero-Diels–Alder elimination of CO₂ under thermal conditions (microwave irradiation), during this elimination the symmetry is increased and out of eight initially possible isomers of the reactant, this number in the product is decreased to four. In oxabicyclo[2.2.2]octene compounds, centrosymmetric hydrogen bonding was found to be the predominant motif and diverse supramolecular patterns were observed due to rich variety of C–H···O and C–H···π interactions.

Keywords: Diels–Alder reaction; X-ray diffraction; organic synthesis; high-pressure conditions; microwave-assisted reactions; heterocycles; hydrogen bonds; aggregation; crystal architecture

1. Introduction

The Diels–Alder reaction, mechanistically classified as a [4+2] cycloaddition belonging to the larger group of pericyclic reactions, is one of the crucial synthetic tools for the construction of novel C–C bonds [1,2], gaining importance in all its varieties, including (organo)catalytic and enantioselective versions [3,4]. Cycloadditions are highly versatile reactions as a broad range of starting dienes and dienophiles (alkenes or alkynes) can be used. Additionally, they are also often highly stereoselective, providing up to four contiguous carbon stereogenic centers and opening access to other stereogenic centers as well, such as chiral phosphorus [5], thus being of paramount importance when a decrease in symmetry (i.e., increase in asymmetry) is desired or necessary as often is the case for the construction of scaffolds of many natural and related compounds. Consequently, cycloadditions provide a viable alternative to the other widespread options of preparing enantiomerically pure compounds, i.e., optical resolution [6] or application of asymmetric (auto)catalysis [7], both of these offering the possibility of enantiomeric excess amplification. There are many empirical rules, partially stemming from the

solid theoretical background set by Woodward and Hoffmann [8–10], which govern regio-, enantio- and diastereoselectivity of cycloadditions. Generally accepted Alder endo rule predicts the formation of the *endo* product as the predominant one. As a consequence of all this, the Diels–Alder reaction is currently in the spotlight of various investigations where amplification of chirality is achieved by dynamic crystallization, an example demonstrated with maleimides and 2-methylfuran (Scheme 1) [11]. Another recent application of cycloaddition reactions, albeit under photochemical conditions, is for the preparation of photochromic organic crystals [12], offering promising properties.

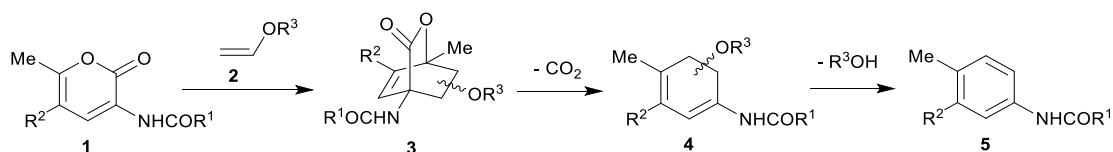


Scheme 1. Highly enantioselective Diels–Alder reactions with 2-methylfuran as diene and *N*-substituted maleimides [11].

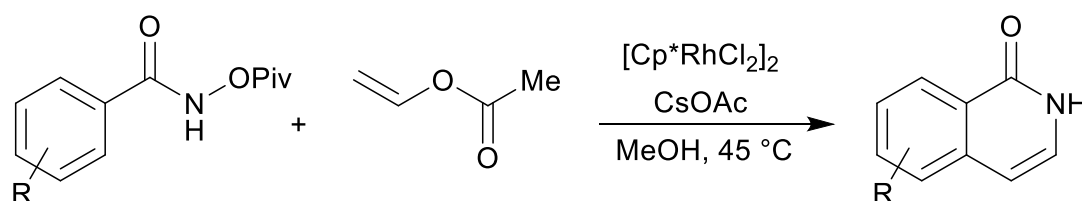
Furthermore, 2*H*-pyran-2-ones are rewarding diene systems capable of many [4+2] cycloaddition reactions [13–15] with a variety of suitable dienophiles, including maleic anhydride, *N*-substituted maleimides, vinyl ethers and their derivatives. The latter type of dienophiles has attracted our attention, as vinyl-group containing compounds can act as reactive partners in [4+2] cycloadditions [16]. Additionally, due to their highly asymmetrical electron density (especially in vinyl ethers and their nitrogen analogs) they can furthermore act as highly regio- and stereoselective partners. For example, in the case of cycloaddition between a substituted 3-acylamino-2*H*-pyran-2-one and ethyl vinyl ether [17] (or any other suitable alkene dienophile), in the first step a carbon-dioxide bridge system (i.e., 7-oxabicyclo[2.2.2]octene) is formed, such systems (including those formed via other reaction pathways) are known from the literature, but their solid-state structures were described just in a few cases, for some recent examples see ref. [18–28]. However, 7-oxabicyclo[2.2.2]octenes produced as described above can be formed as two possible regioisomers and each of these can exist as a mixture of two diastereoisomers (*endo* or *exo*), in turn each of the four distinctive possibilities is actually composed of a pair of enantiomers. Therefore, in a single synthetic step, eight isomeric products (i.e., two regioisomeric compounds each of them as four different stereoisomers) can be formed. However, the reaction can proceed further, via a retro-hetero-Diels–Alder reaction a molecule of carbon dioxide can be eliminated thus producing a cyclohexadiene system, the number of possible isomers is thus reduced to two regioisomers (each of them as a pair of enantiomers). These intermediates can react further via two different pathways. The first option is that an elimination (dehydrogenation in general or elimination of an alcohol in the case of vinyl ethers as dienophiles) takes place yielding the final benzene derivative (only two different regioisomers are possible, stereoisomery obviously not being possible anymore). The second option is that the cyclohexadiene system acts as a new diene and another cycloaddition step takes place (if the dienophile is still available), thus yielding bicyclo[2.2.2]octene systems [29]. Each of their regioisomers can possibly consist of the following stereoisomers: a pair of enantiomers (termed *exo,endo* and *endo,exo*) or one of two different *meso* compounds (*exo,exo* and *endo,endo*). So far all of these possibilities have been achieved [30,31] and various reaction conditions were developed, enabling the preferential formation of the desired products or even of the exact isomers.

Accordingly, many recent investigations have demonstrated that bicyclo[2.2.2]octene adducts are obtained under kinetically controlled reaction conditions, i.e., after shorter reaction times at lower temperatures, in general [32,33]. On the other hand, aromatization of the cyclohexadiene systems can be achieved under thermodynamic conditions and/or with the application of suitable dehydrogenation catalysts (such as active charcoal Darco) or bases (such as DABCO [1,4-diazabicyclo[2.2.2]octane]) when an elimination of a small stable molecule is the objective [34]. To stop the reactions at the first stage, i.e., before the elimination of CO₂, various strategies have been devised, however all of them having in common mild reaction conditions, preferably taking place at room temperature and at increased pressure (up to 18 kbar) [35]. High pressure namely accelerates the cycloaddition step (due to the highly negative activation volume of this step), concomitantly suppressing the elimination of the CO₂ (retro-hetero-Diels–Alder reaction) [36]. Additionally, application of high pressure in organic synthesis has proven to be important, as recently demonstrated by the total synthesis of (–)-aritasone [37], not least because it can lead to changes in regio- and stereoselectivity [38,39].

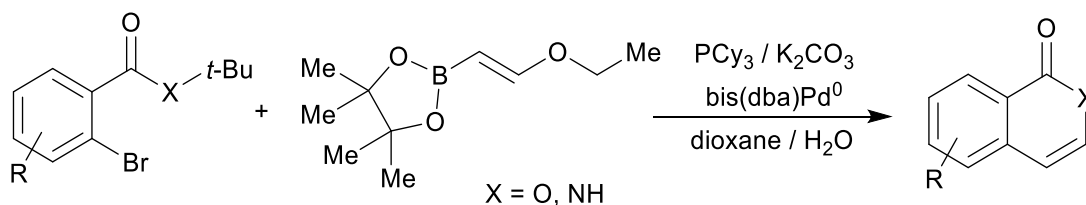
Our previous investigations [16,17] have shown that starting from substituted 2*H*-pyran-2-ones **1** and vinyl-moiety-containing dienophiles **2** the cycloadditions can be selectively directed towards each of the possible products: CO₂-containing 7-oxabicyclo[2.2.2]octenes **3**, cyclohexadienes **4** or final benzene rings **5** (Scheme 2). Furthermore, 7-oxabicyclo[2.2.2]octenes **3** could be prepared only at room temperature under high pressure (13–15 kbar) conditions in dichloromethane (or neat), without the addition of a base. On the other hand, cyclohexadienes **4** were prepared with thermal activation (microwave irradiation in acetonitrile at 120 °C, without a base), whereas the final elimination step to the end products **5** was successfully promoted by the addition of a suitable base, DABCO giving the best results (under microwave irradiation at 120 °C). When the whole reaction sequence (i.e., **1**→**5**) is considered, vinyl ether has acted as a masked acetylene (as its synthetic equivalent, analogously as was previously shown for vinyl acetate (Scheme 3) [40] and vinyl borane (Scheme 4) [41] in other types of reactions), opening further synthetic possibilities as the gaseous acetylene without any electron-perturbing groups generally reacts in Diels–Alder reactions only sluggishly, at best.



Scheme 2. General reaction pathway of a Diels–Alder reaction between 2*H*-pyran-2-one derivatives **1** and vinyl ethers **2** acting as dienophiles.



Scheme 3. Vinyl acetate as a cheap and easy-to-handle synthetic equivalent of explosive and gaseous acetylene [40].



Scheme 4. Vinyl borane as a two-carbon acetylene equivalent applied for the synthesis of isoquinolones (X = NH) and isocoumarins (X = O) [41].

The products thus obtained present some interesting structural characteristics, where the number of isomers possible in each step is decreasing towards the final product **5**, this being consequence of the increase in symmetry as one proceeds from the primary intermediates (i.e., 7-oxabicyclo[2.2.2]octenes **3**) via the cyclohexadiene intermediates **4** towards the final benzene products **5**. Previously, we have revealed just a few X-ray structures of such cases therefore we would now like to report the results of additional single-crystal X-ray characterizations of the products **3** and **4** to determine their structural features including supramolecular aggregation in the solid state form that might influence their properties.

Examination of the number of possible isomers for each of the products obtained when a vinyl ether **2** acts as a dienophile in a Diels–Alder reaction with a substituted 2*H*-pyran-2-one (Figure 1) shows that 7-oxabicyclo[2.2.2]octenes **3**, possessing three stereogenic centers, could theoretically exist as eight different stereoisomers. Due to the steric constraints of the bridged system, both bridgehead stereocenters (i.e., C-1 and C-4) are correlated leading to only four different stereoisomers, distinguished on the base of the configuration of alkoxy groups at the C-8 we get an enantiomeric pair labelled *exo* and another one termed *endo* (meaning that *endo-3* and *exo-3* each exist as a pair of enantiomers). Analogous is the situation with the regioisomeric product **3'**, where alkoxy group is at the position C-7 and can also provide two pairs of enantiomers. Therefore, for all primary adducts **3** and **3'** together, there could be eight different isomers. Upon the elimination of the CO₂, two stereogenic centers (previously C-1 and C-4) are lost, therefore just a pair of enantiomers for each regioisomeric product (i.e., **4** and **4'**) is possible, whereas the final aromatic product **5** can exist only as a single isomer. The situation is analogous when instead of the vinyl ethers **2**, their nitrogen derivatives, such as 1-vinyl-2-pyrrolidone (**6a**) or *N*-vinylcaprolactam (**6b**), are applied and these cases will therefore not be elaborated separately.

Our interest in the above described transformations was initially based on the application of ethyl vinyl ether (and its analogs) as a synthetic equivalent of acetylene for the production of substituted benzene derivatives **5**. This being an interesting application, as it is well-known that acetylene is not a very suitable dienophile in Diels–Alder reactions. Therefore, when we disclosed the results of these syntheses in our previous publications [16,17], the structures of primary cycloadducts (i.e., **3**) and those formed after the elimination of carbon dioxide (i.e., **4**) in the solid state were not of primary importance. Nevertheless, we have investigated [17] the crystal structures of a pair of *exo*- and *endo*-isomers of *N*-[6-acetyl-1-methyl-3-oxo-8-(2-oxoazepan-1-yl)-2-oxabicyclo[2.2.2]oct-5-en-4-yl]benzamide obtained by the cycloaddition between the appropriate 2*H*-pyran-2-one **1a** (R¹ = Ph, R² = Me) and *N*-vinylcaprolactam (**6b**) as the dienophile. X-ray diffraction analysis confirmed that the cycloaddition yielded a mixture of both stereoisomers that we were able to separate and based on the NMR data for these two compounds, the structures of other cycloadducts were established as well. However, we were intrigued by the possibility of further investigating the structures of some of the other cycloadducts of the type **3** and **4** in the solid state, as nowadays novel studies regularly underpin the importance of various intermolecular interactions [42–45], not just hydrogen bonds. Therefore, we prepared suitable crystals of six primary cycloadducts of the type **3** and one cyclohexadiene product **4** and embarked on thorough X-ray crystallographic investigation, including their crystal packing and supramolecular architectures. It turned out that the predominant motif in studied cycloadducts is the intermolecular hydrogen bonding between amide NH group and CO₂ bridge of the adjacent molecule with the domination of centrosymmetric hydrogen-bonded dimers. Furthermore, diverse supramolecular patterns were observed due to rich variety of C–H···O and C–H···π interactions. These supramolecular interactions represent interesting examples of how chiral organic molecules can pack when crystallized as a racemate accommodating a high number of centrosymmetric hydrogen bonds, thus observing symmetry in the crystalline form, albeit the crystals are formed by the aggregation of asymmetric molecules.

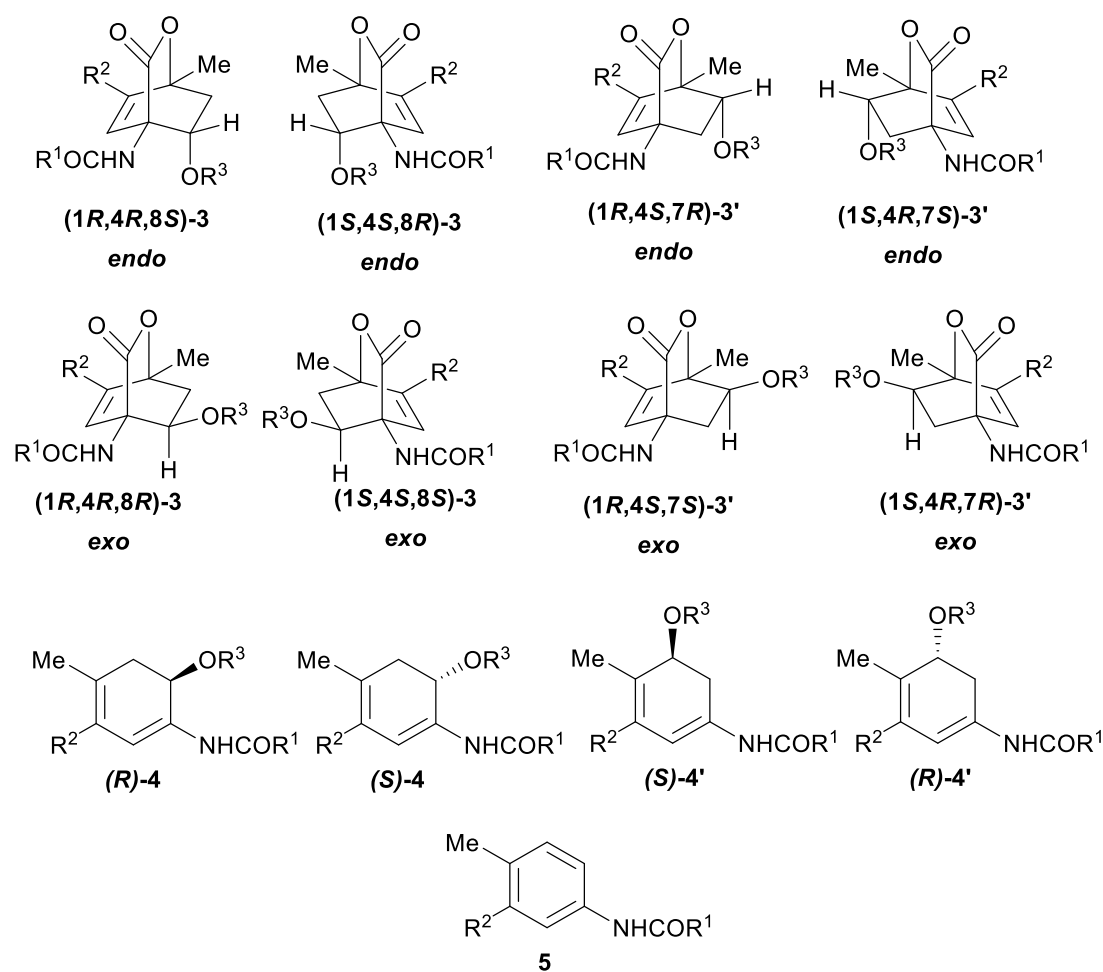


Figure 1. Decreasing number of stereoisomers upon the increase in symmetry of the products (absolute configurations correspond to the following substituents: $R^1 = \text{Ph}$, $R^2 = \text{COMe}$, $R^3 = \text{Et}$).

2. Materials and Methods

2.1. Synthesis

Compounds **3a–e** and **4a** were prepared according to the published procedure [17]. Briefly, adducts **3** were obtained by a high-pressure method conducted in Teflon ampules immersed in a piston-cylinder type of pressure apparatus (U101, Unipress Equipment, Warszawa, Poland) filled with white spirit (also known as mineral spirits) and pressurized at approximately 14 kbar (at room temperature). Reaction mixtures of the appropriate 2*H*-pyran-2-ones **1** (1 equiv.) and dienophiles: ethyl vinyl ether (**2a**) (20 equiv.), cyclohexyl vinyl ether (**2b**) (20 equiv.) or 1-vinyl-2-pyrrolidone (**6a**) (27 equiv.), were diluted with dichloromethane (to completely fill the 3.8 mL ampule) and pressurized for 336–408 h, thereafter the apparatus was disassembled, volatile components were removed in vacuo, crude products **3** precipitated with the addition of isopropyl ether and consequently recrystallized from suitable solvents: methanol for *endo*-**3a**, ethanol for *endo*-**3b–d**, dichloromethane for *exo*-**3e**, isopropyl ether for *exo*-**3f**. Isomer *endo*-**3e** was obtained from the mother liquor after *exo*-**3e** has precipitated. The crystals obtained in all cases were appropriate for X-ray diffraction analyses.

Compound **4a** was prepared by microwave-assisted process in a focused monomode apparatus (Discover by CEM Corporation, Matthews, NC) by irradiation of a mixture of the appropriate 2*H*-pyran-2-one **1f** (1 equiv.) and ethyl vinyl ether (**2a**) (20 equiv.) in acetonitrile (2 mL per mmol of **1**) at 120 °C (180 W) for 2 h, as described previously [17]. After the reaction, product **4a** precipitated upon cooling the mixture in an ice-water bath, filtration and washing with a cold (approximately

0 °C) mixture of ethanol and water (1:1) provided crude cyclohexadiene **4a**, which was carefully recrystallized from ethanol (temperature during the crystallization should not exceed approximately 50–60 °C, as otherwise elimination of ethanol takes place causing partial aromatization of the product) to provide crystals suitable for X-ray diffraction analysis.

2.2. X-ray Single Crystal Analysis

Single-crystal X-ray diffraction data were collected at room temperature on a Nonius Kappa CCD diffractometer with the graphite monochromated Mo-K α radiation ($\lambda = 0.71073 \text{ \AA}$). DENZO program was used to process the data [46]. Structures were solved by direct methods implemented in SHELXS-97 and SHELXL-97 was used for the refinement using a full-matrix least-squares procedure based on F^2 [47]. All non-hydrogen atoms were refined anisotropically. All hydrogen atoms were readily located in difference Fourier maps and were subsequently treated as riding atoms in geometrically idealized positions with $U_{\text{iso}}(\text{H}) = kU_{\text{eq}}(\text{C}, \text{N})$, where $k = 1.5$ for NH and methyl groups, which were permitted to rotate but not to tilt, and 1.2 for all the other H atoms. In *endo-3b* atoms C9–C10 and C24 in each ethoxy group were disordered over two positions with the refined ratios 0.805(19):0.195(19) and 0.444(11):0.556(11), respectively. Atoms C9A, C9B, C10A and C10B were refined with restrained U^{ij} components. Resolution in *endo-3b* is lower than expected; however, the data were of sufficient quality to determine the connectivity. All compounds crystallize as racemates. The crystallographic data are listed in Table 1. The crystallographic data have been deposited at Cambridge Crystallographic Data Centre (CCDC 2034987–2034994) and can be obtained free of charge via www.ccdc.cam.ac.uk/data_request/cif. Appropriate cif-files with single-crystal XRD structures are provided as Supplementary Materials also.

Table 1. Experimental data for the X-ray diffraction studies.

	<i>endo-3a</i>	<i>endo-3b</i>	<i>endo-3c</i>	<i>endo-3d</i>	<i>exo-3e</i>	<i>endo-3e-6a</i>	<i>exo-3f</i>	4a
CCDC number	2034987	2034988	2034989	2034990	2034991	2034992	2034993	2034994
Formula	C ₁₉ H ₂₁ NO ₅	C ₁₄ H ₁₉ NO ₅	C ₁₇ H ₁₉ NO ₆	C ₂₈ H ₂₉ NO ₅	C ₂₄ H ₂₈ N ₂ O ₈	C ₃₀ H ₃₇ N ₃ O ₉	C ₂₆ H ₂₄ N ₂ O ₅	C ₁₈ H ₂₁ NO ₄
<i>M</i> _r (g mol ⁻¹)	343.37	281.3	333.33	459.52	472.48	583.63	444.47	315.36
Crystal size (mm)	0.50 × 0.38 × 0.25	0.25 × 0.25 × 0.25	0.70 × 0.50 × 0.50	0.45 × 0.25 × 0.20	0.35 × 0.10 × 0.10	0.50 × 0.13 × 0.13	0.60 × 0.30 × 0.18	0.50 × 0.20 × 0.20
Crystal color	colorless	colorless	colorless	colorless	colorless	colorless	colorless	colorless
Crystal system	orthorhombic	triclinic	orthorhombic	monoclinic	monoclinic	triclinic	triclinic	orthorhombic
Space group	<i>Pcab</i>	<i>P</i> -1	<i>Pcab</i>	<i>C2/c</i>	<i>P2</i> ₁ / <i>n</i>	<i>P</i> -1	<i>P</i> -1	<i>Pcab</i>
<i>a</i> (Å)	13.6258(2)	11.1004(9)	13.2171(2)	25.6982(6)	10.1996(4)	11.2314(3)	9.2483(3)	12.1827(3)
<i>b</i> (Å)	15.0585(3)	11.3611(8)	14.2221(3)	13.3577(2)	19.6440(11)	11.6094(3)	11.4819(3)	14.8081(4)
<i>c</i> (Å)	17.0887(3)	13.2166(9)	17.1809(4)	18.3592(4)	12.5325(6)	12.1689(3)	12.1508(3)	18.6214(4)
α (°)	90	65.350(3)	90	90	90	85.027(2)	112.763(2)	90
β (°)	90	89.871(4)	90	127.2900(10)	113.734(3)	73.439(2)	93.341(2)	90
γ (°)	90	81.713(3)	90	90	90	78.714(2)	106.199(2)	90
<i>V</i> (Å ³)	3506.33(11)	1495.97(19)	3229.58(11)	5013.85(18)	2298.65(19)	1490.66(7)	1122.23(5)	3359.35(14)
<i>Z</i>	8	4	8	8	4	2	2	8
<i>T</i> (K)	293(2)	293(2)	293(2)	293(2)	293(2)	293(2)	293(2)	293(2)
<i>D</i> _c (g cm ⁻³)	1.301	1.249	1.371	1.218	1.365	1.300	1.315	1.247
<i>F</i> (000)	1456	600	1408	1952	1000	620	468	1344
Reflections collected	7555	6695	6922	10443	8146	12041	8995	7151
<i>R</i> _{int}	0.0132	0.0459	0.0143	0.0192	0.0551	0.0232	0.0271	0.0285
Data/restraints/parameters	3990/0/230	3976/38/402	3663/0/221	5708/0/309	4170/0/313	6796/0/385	5103/0/300	3783/0/212
<i>R</i> ₁ , <i>wR</i> ₂ [<i>I</i> > 2σ(<i>I</i>)] ^a	0.0442, 0.1092	0.0576, 0.1418	0.0471, 0.1293	0.0551, 0.1413	0.0573, 0.1252	0.0482, 0.1219	0.0535, 0.1356	0.0586, 0.1431
<i>R</i> ₁ , <i>wR</i> ₂ (all data) ^b	0.0595, 0.1206	0.0926, 0.1650	0.0618, 0.1429	0.0874, 0.1683	0.1184, 0.1572	0.0715, 0.1385	0.0768, 0.1547	0.0940, 0.1709
<i>GOF</i> , <i>S</i> ^c	1.050	1.040	1.044	1.023	1.038	1.017	1.025	1.046

^a $R = \sum |F_o| - |F_c| / \sum |F_o|$. ^b $wR_2 = \{\sum [w(F_o^2 - F_c^2)^2] / \sum [w(F_o^2)^2]\}^{1/2}$. ^c $S = \{\sum [(F_o^2 - F_c^2)^2] / (n/p)\}^{1/2}$ where *n* is the number of reflections and *p* is the total number of parameters refined.

3. Results

3.1. Chemistry

As presented in Table 2, crystals suitable for X-ray diffraction were prepared for the following oxabicyclo[2.2.2]octene products [17]: (i) set of three *endo* adducts **3a–c** obtained with the cycloaddition of ethyl vinyl ether (**2a**) on the appropriate *2H*-pyran-2-ones **1a–c**; (ii) for *endo-3d* obtained by the cycloaddition of cyclohexyl vinyl ether (**2b**) on *2H*-pyran-2-one **1d**; (iii) for the pair of *endo* and *exo* adducts **3e** produced by the cycloaddition of 1-vinyl-2-pyrrolidone (**6a**) on the *2H*-pyran-2-one **1e**; (iv) for the *exo-3f* obtained by the cycloaddition between **6a** and *2H*-pyran-2-one **1d**. Additionally, a single crystal of cyclohexadiene product **4a** was also prepared; however, in contrast to the high-pressure conditions appropriate for the preparation of **3**, here thermal activation with microwaves was necessary. Microwave irradiation as a way to facilitate organic reactions has during the last decades found some surprisingly widespread applications, as recently vividly described by Kappe [48], including acceleration of Diels–Alder reactions [2,49], Kabachnik–Fields reaction [50] and many others.

Table 2. Prepared products [17].

Run	Starting <i>2H</i> -pyran-2-ones 1		Dienophile	R ³	Reaction Time	Product	Yield (%) ^a	Solvent for Crystallization	
	R ¹	R ²							
1	Ph	Me	1a	2a	Et	336 h ^b	<i>endo-3a</i>	73	MeOH
2	Me	Me	1b	2a	Et	408 h ^b	<i>endo-3b</i>	66	EtOH
3	2-furyl	Me	1c	2a	Et	384 h ^b	<i>endo-3c</i>	70	EtOH
4	Ph	Ph	1d	2b	cyclohexyl	408 h ^b	<i>endo-3d</i>	65	EtOH
5	3,4,5-(OMe) ₃ -C ₆ H ₂ -	Me	1e	6a	2-oxopyrrolidin-1-yl	408 h ^b	<i>exo-3e</i>	68	CH ₂ Cl ₂
6	3,4,5-(OMe) ₃ -C ₆ H ₂ -	Me	1e	6a	2-oxopyrrolidin-1-yl	384 h ^b	<i>endo-3e</i>	0.5	CH ₂ Cl ₂
7	Ph	Ph	1d	6a	2-oxopyrrolidin-1-yl	384 h ^b	<i>exo-3f</i>	68	<i>i</i> -Pr ₂ O
8	Ph	OMe	1f	2a	Et	2 h ^c	4a	35	EtOH

^a Yield of isolated products. ^b In CH₂Cl₂ at high pressure (approximately 14 kbar) at room temperature. ^c Under microwave irradiation at 120 °C (180 W).

It is worth noting that product *endo-3e* was isolated by precipitation upon slow evaporation of the volatile components from the mother liquor (which remained after the precipitation of *exo-3e* and its removal by vacuum filtration) containing an appreciable amount of the starting dienophile **6a** (which was initially applied in a large excess, also as a co-solvent, in molar ratio **1e:6a** = 1:27). Consequently, *endo* isomer was found to crystallize as a solvate *endo-3e-6a*.

3.2. X-Ray Single Crystal Determination

Compounds *endo-3a* and *endo-3c* crystallize in the orthorhombic space group *Pcab*, compound *endo-3d* in the monoclinic space group *C2/c* and compound *exo-3e* in the monoclinic space group *P2₁/n* while compounds *endo-3b*, *endo-3e* and *exo-3f* crystallize in the triclinic space group *P-1*. Compound **4a** crystallizes in the orthorhombic space group *Pcab*. In all crystal structures asymmetric units are composed of one molecule except in *endo-3b* where two crystallographically independent molecules are present in the asymmetric unit and in *endo-3e-6a* where the asymmetric unit is composed of a molecule *endo-3e* and a molecule of 1-vinyl-2-pyrrolidone (**6a**) as a solvate. Crystal structures are presented in Figure 2.

Compounds **3** possess rigid 7-oxabicyclo[2.2.2]octene skeleton and thus structures variate primarily due to different substituents at the position 6 (acetyl, benzoyl), 8 (cyclohexyloxy, ethoxy, 2-oxopyrrolidin-1-yl) and 4 (benzoylamino, acetylamino, trimethoxybenzoylamino, furan-2-carboxylamino) while position 1 is always occupied by a methyl group. Different substituents present at positions 4, 6 and 8 enable diverse interactions in the crystal structure. All compounds possess one classical hydrogen bond donor, namely amide NH group. On the other hand, there are several potential hydrogen bond acceptors, such as oxygen atoms of side arms at the positions 4, 6 and 8 as well as both oxygen atoms in the CO₂ bridge.

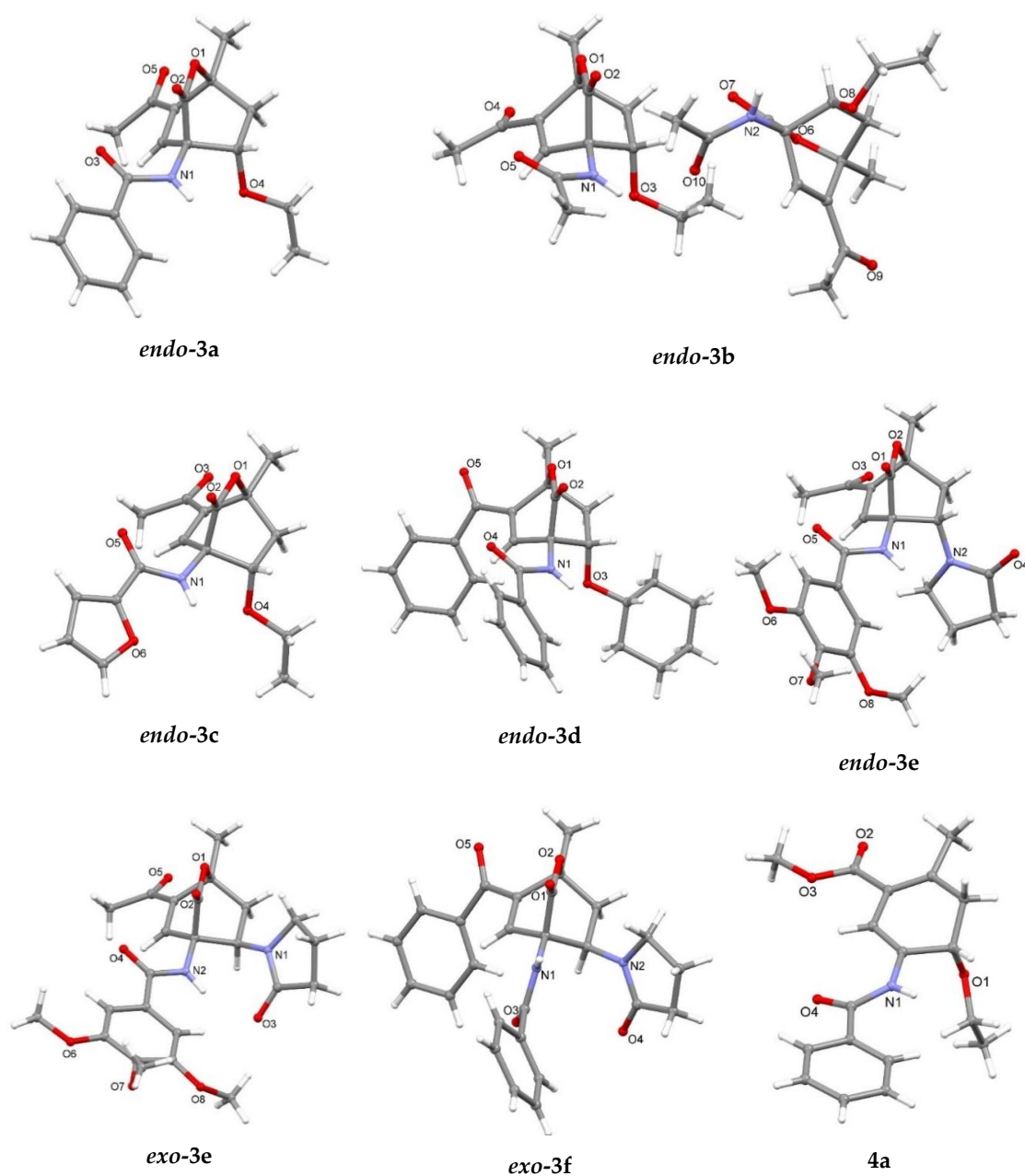


Figure 2. Crystal structures of 7-oxabicyclo[2.2.2]octenes **3a–f** and cyclohexadiene **4a**. In *endo-3b* two crystallographic molecules are present in the asymmetric unit, disorder is omitted for clarity. In *endo-3e*, solvate molecule **6a** is omitted for clarity.

In compound *endo-3a*, hydrogen-bonded centrosymmetric dimer is formed via $N1-H1 \cdots O2^i$ interaction between the amide NH group acting as a hydrogen bond donor and the carbonyl oxygen atom of the CO_2 bridge of the symmetry related molecule as a hydrogen bond acceptor with the graph-set motif $R_2^2(10)$ [51] (Figure 3a, Table 3). This interaction is further supported by centrosymmetric $C4-H4b \cdots \pi$ interaction between the bicyclo[2.2.2]octene scaffold and the phenyl ring of the benzoylamino substituent with $d(H4b \cdots Cg4) = 2.83 \text{ \AA}$ and $\angle(C4-H4b \cdots Cg4) = 155^\circ$, where $Cg4$ is C14–C19 ring centroid. Dimeric structure is further connected into a layer along the *ab* plane via $C9-H9c \cdots \pi$ interaction between acetyl moiety and phenyl ring of the benzoylamino substituent of the adjacent hydrogen-bonded dimer (Figure 3b–d). There are no significant $\pi \cdots \pi$ interactions.

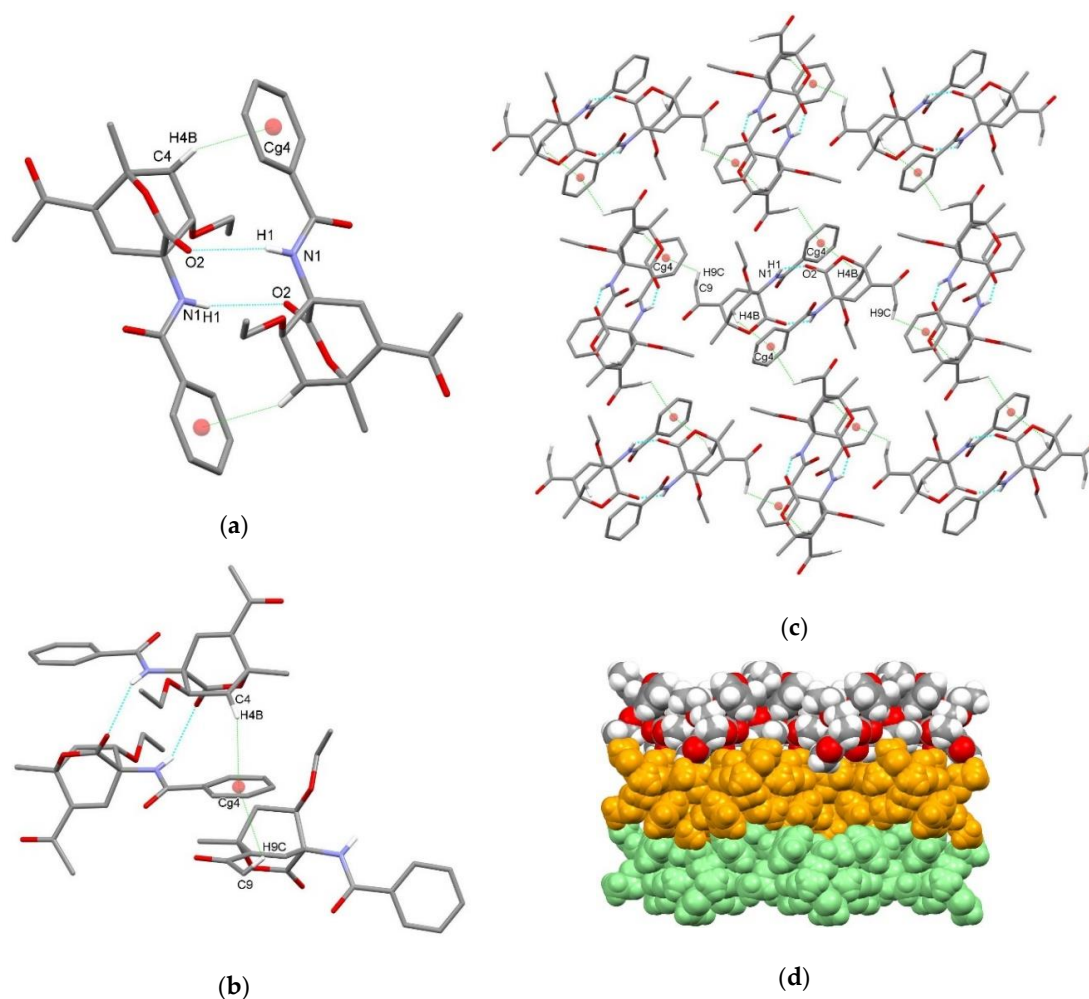


Figure 3. Supramolecular aggregation of *endo-3a*. (a) Hydrogen-bonded centrosymmetric dimer formed through N-H...O and C-H...π interactions; (b) hydrogen-bonded dimers are further connected with adjacent dimers through C-H...π interactions forming (c) layer; (d) packing of layers (arbitrary colors). Hydrogen atoms not involved in the motifs shown have been omitted for clarity.

Table 3. Hydrogen bonds for **3a–f** and **4a** [Å and °].

D–H...A	<i>d</i> (D–H)	<i>d</i> (H...A)	<i>d</i> (D...A)	(DHA)
<i>endo-3a</i>				
N1–H1...O2 ⁱ	0.86	2.31	3.0684(15)	147.2
<i>endo-3b</i>				
N1–H29...O10	0.86	2.32	2.937(3)	128.7
N2–H30...O2 ⁱ	0.86	2.06	2.909(3)	170.1
C1–H1...O7	0.98	2.33	3.223(4)	152
C12–H12A...O9 ⁱⁱ	0.96	2.60	3.528(6)	163
C16–H16B...O7 ⁱⁱⁱ	0.97	2.57	3.482(5)	157
C28–H28A...O2	0.96	2.59	3.461(5)	151
<i>endo-3c</i>				
N1–H1...O2 ⁱ	0.86	2.33	3.1063(17)	151
C16–H16...O5 ⁱⁱ	0.93	2.51	3.369(2)	154

Table 3. Cont.

D–H···A	d(D–H)	d(H···A)	d(D···A)	(DHA)
endo-3d				
N1–H1···O2 ⁱ	0.86	2.36	3.121(2)	148.3
C11–H11···O4 ⁱⁱ	0.93	2.49	3.363(5)	157
C18–H18A···O4 ⁱⁱⁱ	0.97	2.56	3.471(3)	157
C27–H27···O1 ^{iv}	0.93	2.48	3.350(3)	156
endo-3e-6a				
N1–H1···O4 ⁱ	0.86	2.08	2.8979(16)	158.6
C3–H3···O8 ⁱⁱ	0.93	2.56	3.490(2)	174
C9–H9C···O8 ⁱⁱ	0.96	2.60	3.536(2)	166
C27–H27A···O1	0.97	2.51	3.216(3)	130
C27–H27B···O5 ⁱⁱⁱ	0.97	2.60	3.287(3)	128
exo-3e				
N2–H2···O3	0.86	2.10	2.891(3)	152.9
C10–H10C···O7 ⁱ	0.96	2.36	3.242(5)	152
C22–H22A···O3 ⁱ	0.96	2.49	3.323(4)	145
C23–H23C···O6 ⁱⁱ	0.96	2.47	3.424(5)	171
exo-3f				
N1–H1···O1 ⁱ	0.86	2.32	3.0620(18)	145.2
C12–H12···O5 ⁱⁱ	0.93	2.32	3.198(6)	157
C19–H19B···O4 ⁱⁱⁱ	0.96	2.58	3.439(3)	149
4a				
N1–H1···O2 ⁱ	0.86	2.28	2.923(3)	131.6
C6–H6···O2 ⁱ	0.98	2.57	3.313(3)	133
C18–H18···O4 ⁱⁱ	0.93	2.52	3.375(3)	152

Symmetry codes for **endo-3a**: (i) $-x + 1, -y + 2, -z + 2$; for **endo-3b**: (i) $-x, -y + 1, -z + 1$; (ii) $x - 1, y + 1, z$; (iii) $-x + 1, -y + 1, -z + 1$; for **endo-3c**: (i) $-x + 1, -y, -z$; (ii) $x + \frac{1}{2}, -y, -z - \frac{1}{2}$; for **endo-3d**: (i) $-x, -y + 1, -z$; (ii) $-x - \frac{1}{2}, y - \frac{1}{2}, -z - \frac{1}{2}$; (iii) $x + \frac{1}{2}, -y + \frac{1}{2}, z + \frac{1}{2}$; (iv) $x, -y + 1, z + \frac{1}{2}$; for **endo-3e-6a**: (i) $-x, -y + 1, -z + 2$; (ii) $-x + 1, -y + 1, -z + 2$; (iii) $-x + 1, -y + 1, -z + 1$; for **exo-3e**: (i) $-x, -y + 2, -z + 1$; (ii) $-x, -y + 2, -z + 2$; for **exo-3f**: (i) $-x + 1, -y + 1, -z + 2$; (ii) $x + 1, y + 1, z + 1$; (iii) $-x + 1, -y + 1, -z + 1$; for **4a**: (i) $x, y - \frac{1}{2}, -z + 3/2$; (ii) $-x + 1, -y + 2, -z + 2$.

In compound **endo-3b**, hydrogen-bonded centrosymmetric tetramer is present, formed via a combination of N1–H29···O10 and N2–H30···O2ⁱ interactions with the graph-set motif $R_4^4(18)$. In this tetramer, molecule A forms a hydrogen bond through the amide NH group acting as a hydrogen bond donor with the carbonyl oxygen atom of the amide group of molecule B acting as a hydrogen bond acceptor. Furthermore, molecule B forms a hydrogen bond through amide NH group acting as a hydrogen bond donor with the carbonyl oxygen atom of the CO₂ bridge of symmetry related molecule A acting as a hydrogen bond acceptor (Figure 4a, Table 3). Tetramer is further supported by C1–H1···O7 interaction between the bicyclo[2.2.2]octene scaffold of molecule A and the carbonyl oxygen atom of the CO₂ bridge of molecule B, as well as C28–H28A···O2 interaction between methyl group of acetylamino substituent of molecule B and the carbonyl oxygen atom of the CO₂ bridge of molecule A. Tetramers are further connected into layers along the *ab* plane via C12–H12A···O9ⁱⁱ and C16–H16B···O7ⁱⁱⁱ interactions (Figure 4b). There are no significant C–H··· π and π ··· π interactions.

In compound **endo-3c**, hydrogen-bonded centrosymmetric dimer is formed via N1–H1···O2ⁱ interaction between the amide NH group acting as a hydrogen bond donor and the carbonyl oxygen atom of the CO₂ bridge of the adjacent molecule as a hydrogen bond acceptor with the graph-set motif $R_2^2(10)$ (Figure 5a, Table 3). Dimers are further connected into 3D structure due to C–H···O and C=O··· π interactions. C16–H16···O5ⁱⁱ interactions enable the formation of layers along the *ac* plane between furyl ring and carbonyl oxygen atom of the furan-2-carboxylamino substituent of the adjacent hydrogen-bonded dimer (Figure 5b), while C9=O3··· π interactions between the acetyl moiety and the furyl ring of the adjacent hydrogen-bonded dimer enable the formation of layers along the *ab* plane

with $d(\text{O}3 \cdots \text{Cg}1) = 3.5759(19) \text{ \AA}$ and $\angle(\text{C}9=\text{O}3 \cdots \text{Cg}1) = 74.16(11)^\circ$, where $\text{Cg}1$ is $\text{O}6/\text{C}14\text{--C}17$ ring centroid (Figure 5c). There are no significant $\pi \cdots \pi$ interactions.

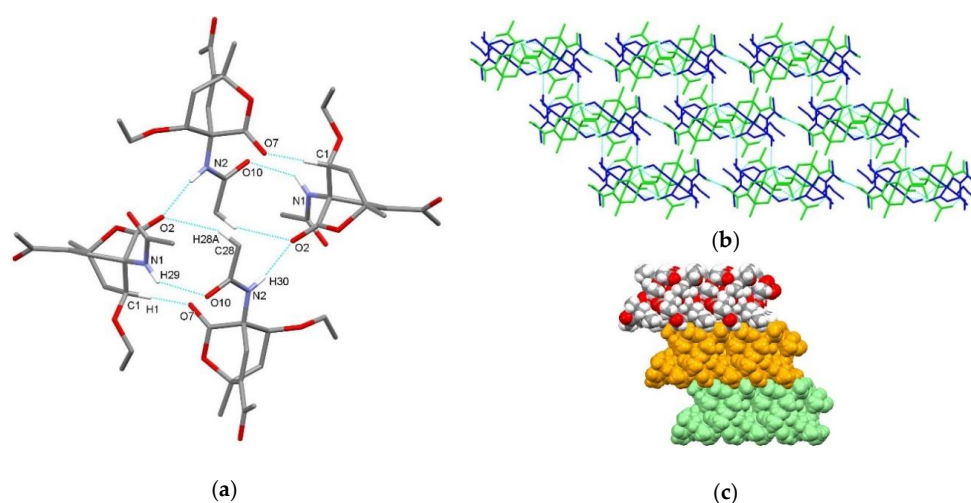


Figure 4. Supramolecular aggregation of *endo-3b*. (a) Hydrogen-bonded centrosymmetric tetramer formed through $\text{N-H} \cdots \text{O}$ and $\text{C-H} \cdots \text{O}$ interactions; (b) layer formation connecting tetramers through $\text{C-H} \cdots \text{O}$ interactions (color code: symmetry equivalents); (c) packing of layers (arbitrary colors). Hydrogen atoms not involved in the motifs shown and disorder have been omitted for clarity.

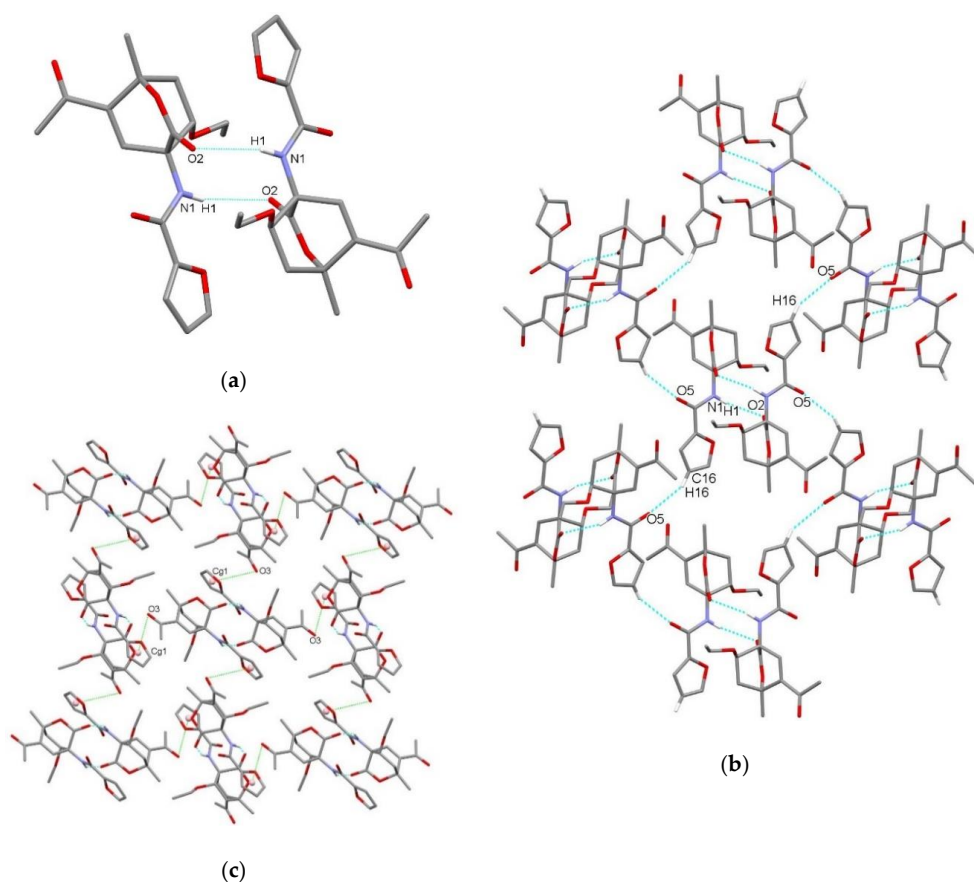


Figure 5. Supramolecular aggregation of *endo-3c*. (a) Hydrogen-bonded centrosymmetric dimer formed through $\text{N-H} \cdots \text{O}$ interaction; (b) layer formation along ac plane through the $\text{C-H} \cdots \text{O}$ interactions; (c) layer formation along ab plane through the $\text{C}=\text{O} \cdots \pi$ interactions. Hydrogen atoms not involved in the motifs shown have been omitted for clarity.

In compound *endo-3d*, hydrogen-bonded centrosymmetric dimer is formed via $N1-H1 \cdots O2^i$ interaction between the amide NH group acting as a hydrogen bond donor and the carbonyl oxygen atom of the CO_2 bridge of the adjacent molecule as a hydrogen bond acceptor with the graph-set motif $R_2^2(10)$ (Figure 6a, Table 3). This interaction is further supported by centrosymmetric $C4-H4b \cdots \pi$ interaction between the bicyclo[2.2.2]octene scaffold and the phenyl ring of the benzoylamino substituent with $d(H4b \cdots Cg6) = 2.92 \text{ \AA}$ and $\angle(C4-H4b \cdots Cg6) = 149^\circ$, where $Cg6$ is C23–C28 ring centroid. Dimers are further connected into layers along the (-101) plane through the combination of $C11-H11 \cdots O4^{ii}$ and $C18-H18a \cdots O4^{iii}$ interactions connecting phenyl ring of benzoylamino moiety and cyclohexyl substituent, both as hydrogen bond donors, with the carbonyl oxygen atom of the amide group of two different adjacent molecules (Figure 6b), thus carbonyl O4 atom acts as an acceptor of two hydrogen bonds from two different adjacent molecules. Three-dimensional supramolecular structure is achieved through the $C27-H27 \cdots O1^{iv}$ interactions along c axis between the phenyl ring of benzoylamino moiety and the ring oxygen atom of the CO_2 bridge (Figure 6c). There are no significant $\pi \cdots \pi$ interactions.

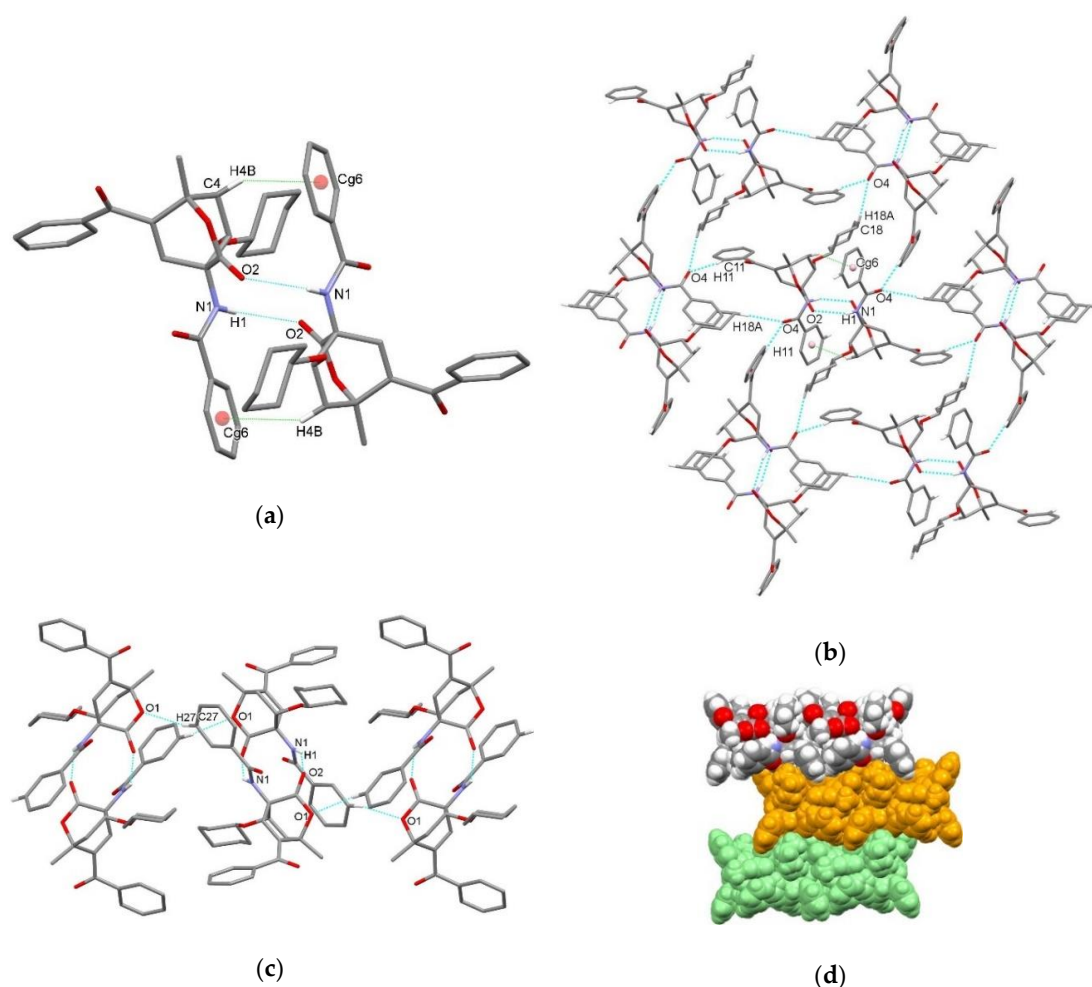


Figure 6. Supramolecular aggregation of *endo-3d*. (a) Hydrogen-bonded centrosymmetric dimer formed through $N-H \cdots O$ and $C-H \cdots \pi$ interactions; (b) hydrogen-bonded dimers connected into layer through $C-H \cdots O$ interactions ($C-H \cdots \pi$ interactions within a dimer are presented only for the central one); (c) $C-H \cdots O$ interactions between dimers along c axis; (d) packing of layers (arbitrary colors). Hydrogen atoms not involved in the motifs shown have been omitted for clarity.

In compound *endo-3e-6a*, hydrogen-bonded centrosymmetric dimer is formed via $N1-H1 \cdots O4^i$ interaction between the amide NH group acting as a hydrogen bond donor and the carbonyl oxygen atom of the 2-oxopyrrolidin-1-yl group of the adjacent molecule as a hydrogen bond acceptor with the graph-set motif $R_2^2(14)$ (Figure 7a, Table 3). Dimers are further connected into chains along *a* axis through the combination of centrosymmetric $C3-H3 \cdots O8^{ii}$ and $C9-H9c \cdots O8^{ii}$ interactions connecting acetyl moiety and bicyclo[2.2.2]octene scaffold, both as hydrogen bond donors, with the methoxy oxygen atom of the trimethoxybenzoylamino group of the adjacent molecule, thus methoxy O8 atom acts as an acceptor of two hydrogen bonds from one adjacent molecule (Figure 7a). Interactions between hydrogen-bonded chains of *3e* and solvate molecules *6a* enable the formation of layers through the $C27-H27a \cdots O1$ and $C27-H27b \cdots O5^{iii}$ interactions composed of centrosymmetric hydrogen-bonded tetramer with ABAB pattern with the graph-set motif $R_4^4(18)$ (Figure 7b). There are no significant $C-H \cdots \pi$ and $\pi \cdots \pi$ interactions.

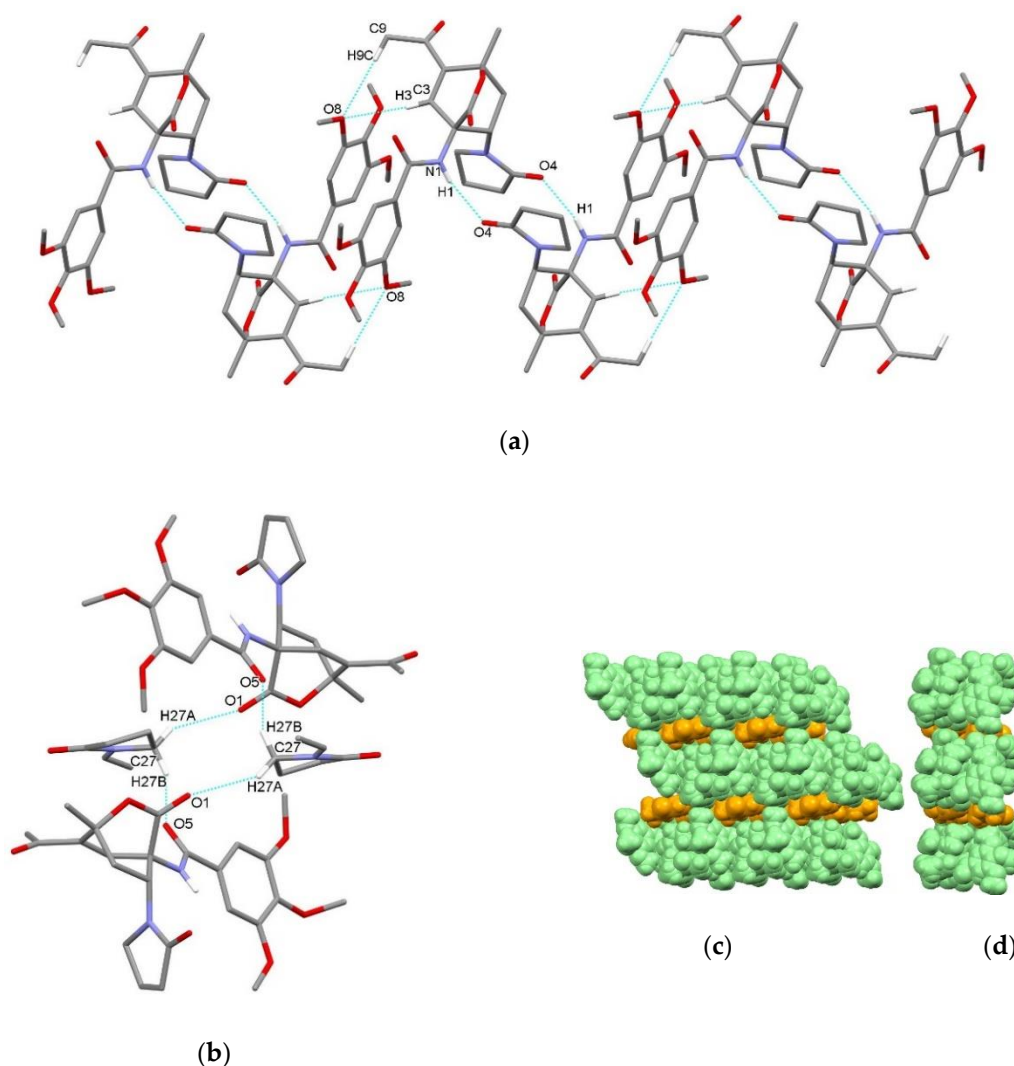


Figure 7. Supramolecular aggregation of *endo-3e-6a*. (a) Hydrogen-bonded centrosymmetric dimers formed through $N-H \cdots O$ interactions are further connected through centrosymmetric $C-H \cdots O$ interactions; (b) centrosymmetric hydrogen-bonded tetramer composed of two *endo-3e* molecules and two solvate molecule connected through $C-H \cdots O$ interactions; packing of chains of *endo-3e* (green) and 1-vinyl-2-pyrrolidone (*6a*) solvate molecules (orange) (c) front and (d) side view. Hydrogen atoms not involved in the motifs shown have been omitted for clarity.

In compound *exo-3e*, amide NH group is not involved in intermolecular hydrogen bonding; however, it forms intramolecular N2–H2···O3 interaction with the carbonyl oxygen atom of the 2-oxopyrrolidin-1-yl substituent. However, centrosymmetric dimer is still formed, in this case via C10–H10c···O7ⁱ interaction between acetyl substituent and methoxy group of trimethoxybenzoylamino substituent and via C22–H22a···O3ⁱ interaction between methoxy group and the 2-oxopyrrolidin-1-yl oxygen atom with the graph-set motifs R₂²(16) and R₂²(26) (Figure 8a, Table 3). Furthermore, dimers connect into a chain along *c* axis via centrosymmetric C23–H23c···O6ⁱⁱ interaction between methoxy groups of two adjacent molecules (Figure 8a). There are no significant C–H··· π and π ··· π interactions.

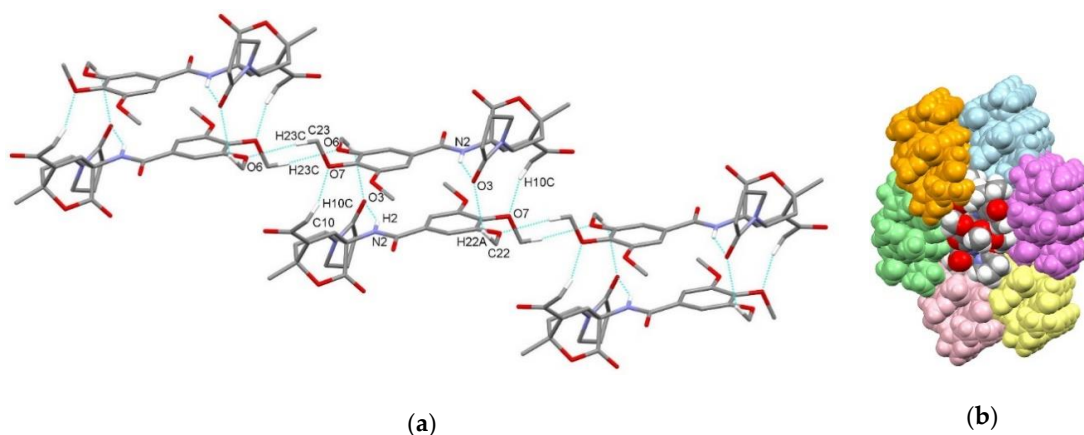


Figure 8. Supramolecular aggregation of *exo-3e*. (a) Hydrogen-bonded centrosymmetric dimers formed through C–H···O interactions extended into chain through additional centrosymmetric C–H···O interactions; (b) packing of chains (color code: arbitrary colors). Hydrogen atoms not involved in the motifs shown have been omitted for clarity.

In compound *exo-3f*, hydrogen-bonded centrosymmetric dimer is formed via N1–H1···O1ⁱ interaction between the amide NH group acting as a hydrogen bond donor and the carbonyl oxygen atom of the CO₂ bridge of the adjacent molecule as a hydrogen bond acceptor with the graph-set motif R₂²(10). Dimers are further connected into chain along *c* axis through centrosymmetric C19–H19b···O4ⁱⁱ interactions connecting methyl substituent at the bicyclo[2.2.2]octene skeleton with the carbonyl oxygen atom of the 2-oxopyrrolidin-1-yl substituent of the adjacent molecule with the graph-set motif R₂²(16) (Figure 9a, Table 3). Chains are further connected into a layer along the (−110) plane through C12–H12···O5ⁱⁱⁱ interactions between the phenyl ring of benzoylamino group and the carbonyl oxygen atom of the benzoyl unit (Figure 9b). There are no significant C–H··· π and π ··· π interactions.

Compound **4a** represents a very rare case of a cyclohexadiene system stable at room temperature, albeit containing groups that are prone to elimination (in this case of a molecule of ethanol), which would furnish a benzene derivative, thus achieving aromatic stabilization. Another case from the literature was described by Afarinkia et al. [52]. In compound **4a**, hydrogen-bonded chain along *b* axis is formed via $N1-H1 \cdots O2^i$ interaction between the amide NH group acting as a hydrogen bond donor and the carbonyl oxygen atom of the ester group of the adjacent molecule as a hydrogen bond acceptor supported by $C6-H6 \cdots O2^i$ interaction forming graph-set motif $R_1^2(6)$ (Figure 10a, Table 3). Chains are further connected into a zig-zag layer along *bc* plain through centrosymmetric $C18-H18 \cdots O4^{ii}$ interactions between benzoylamino substituents of adjacent molecules with graph-set motif $R_2^2(10)$ (Figure 10b). There are no significant $C-H \cdots \pi$ and $\pi \cdots \pi$ interactions.

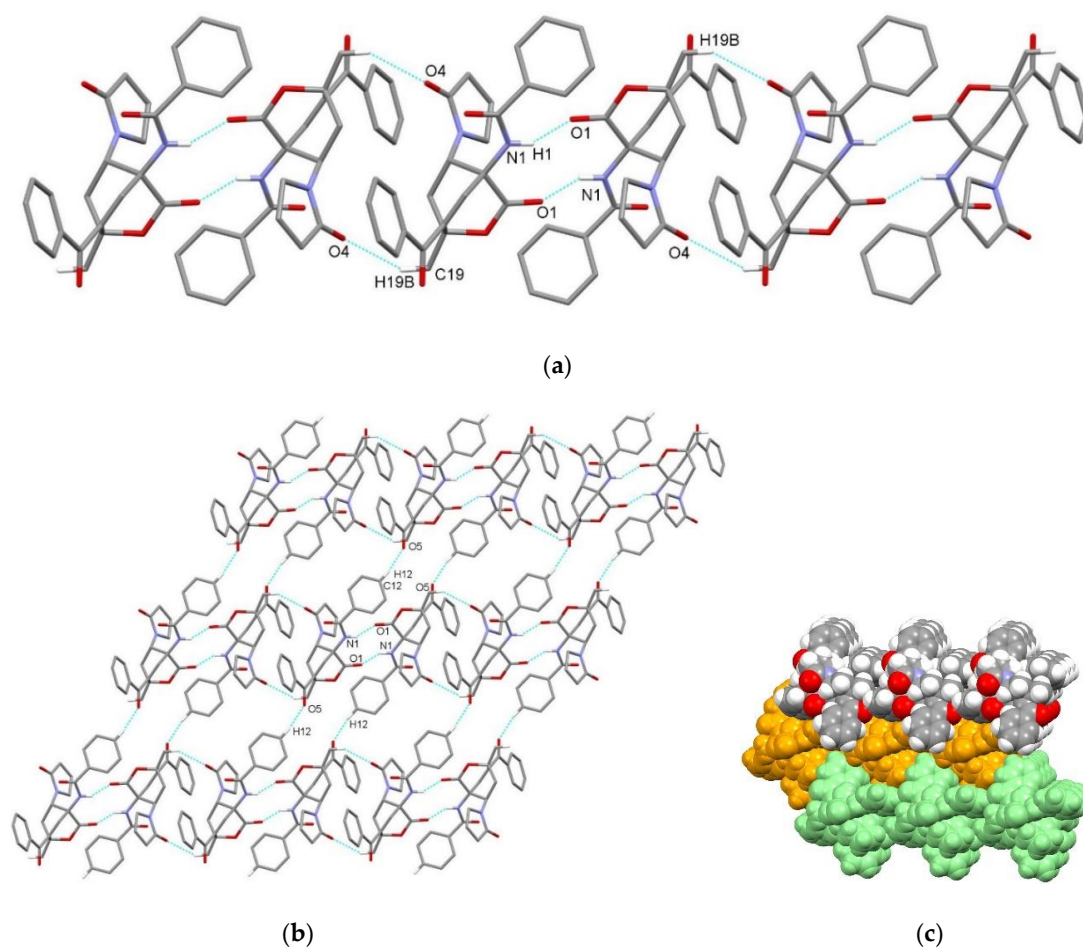


Figure 9. Supramolecular aggregation of *exo*-3f. (a) Hydrogen-bonded chain formed through centrosymmetric $N-H \cdots O$ and $C-H \cdots O$ interactions; (b) chains connected into a layer through $C-H \cdots O$ interactions; (c) packing of layers (color code: arbitrary colors). Hydrogen atoms not involved in the motifs shown have been omitted for clarity.

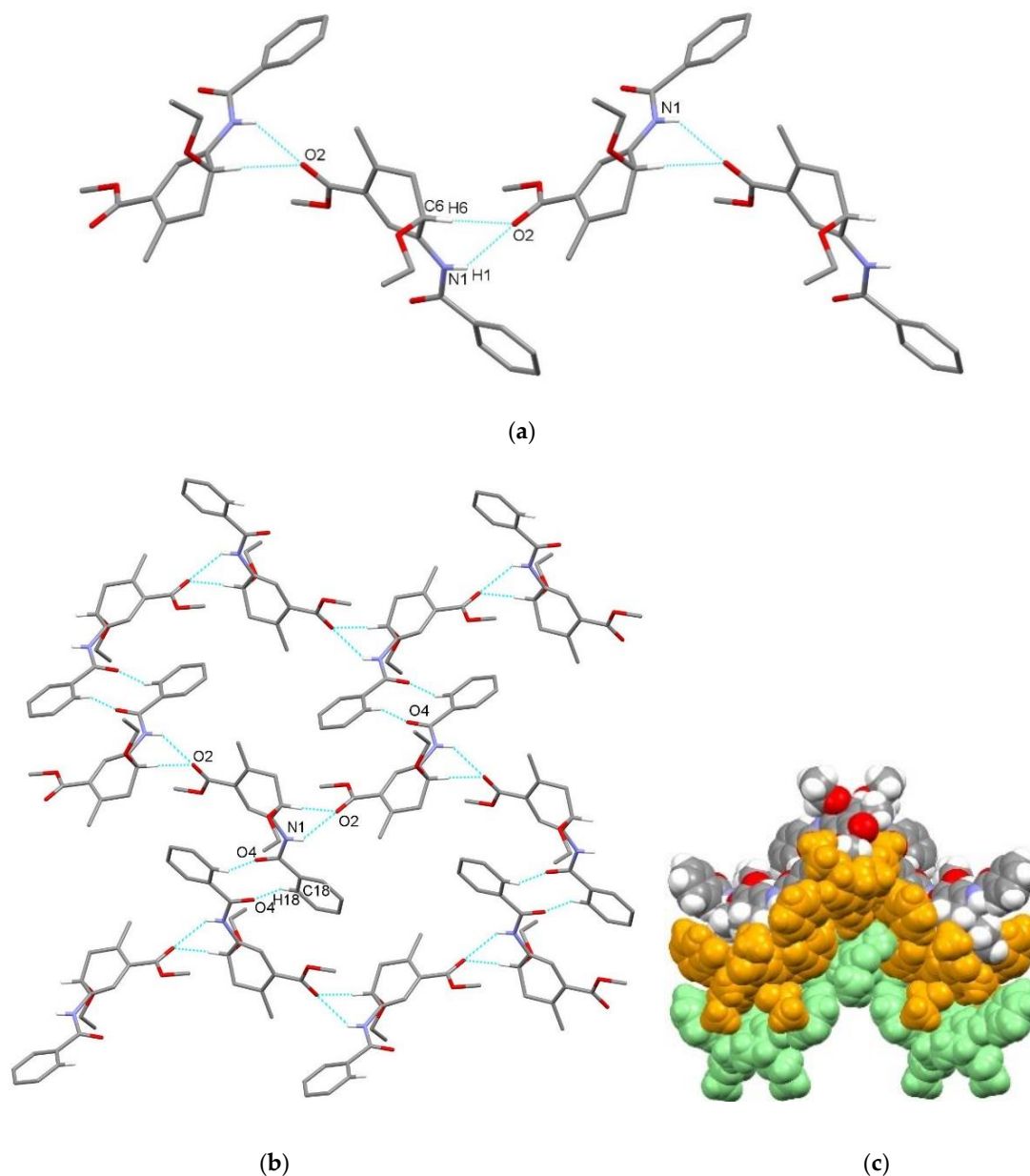


Figure 10. Supramolecular aggregation of **4a**. (a) Hydrogen-bonded chain formed through N–H···O and C–H···O interactions; (b) chains connected into a layer through centrosymmetric C–H···O interactions; (c) packing of zig-zag layers (color code: arbitrary colors). Hydrogen atoms not involved in the motifs shown have been omitted for clarity.

4. Discussion

We have demonstrated that the cycloadditions between 2*H*-pyran-2-one derivatives **1a–e** and various vinyl-moiety-containing dienophiles **2** and **6** in the first step yield oxabicyclo[2.2.2]octene products of the type **3**. However, the reaction can be successfully stopped at this step only if it is taking place under mild conditions, temperatures above approximately 50–60 °C cause immediate and irreversible elimination of carbon dioxide via retro-hetero-Diels–Alder reaction and thus cyclohexadiene systems **4** are formed. However, the cycloadditions are sluggish, at best, at ambient conditions, therefore we found that the only possibility to obtain products **3** was to avoid thermal activation of the reaction and instead use activation with high pressure [35,36,39], which is known to accelerate processes having negative activation volumes (among such processes are generally all reactions where two molecules give just one; however, the solvation effects have to be considered as well). Empirically it was established

that the majority of Diels–Alder reactions indeed possess negative activation volumes [53,54] and are therefore prone to be accelerated under high pressure conditions. As cycloadditions are equilibrium processes, we applied large excess of the dienophile **2** to push the position of the equilibrium towards the products **3**; however, due to the practical reasons of solubility (and to decrease the viscosity), some dichloromethane as a solvent was also necessary.

We have to stress that the crystal structures of the products **3** presented herein are the only 7-oxabicyclo[2.2.2]octenes possessing a substituted amino group at one of the bridgehead atoms described so far, in addition to one publication (describing three structures) by Haufe et al., [22] and our own previous report [17]. It is interesting to note that in all cases where oxygen-based dienophiles **2** (i.e., **2a,b**) were used, the only stereoisomer of the products **3** obtained was of the *endo* type; however, with the nitrogen-based dienophile (i.e., **6a**) in one case (i.e., formation of **3f**) only *exo* stereoisomer was obtained, whereas in the other case (i.e., formation of **3e**) a mixture of both *endo* and *exo* stereoisomers was produced. Obviously, all of the products were obtained as racemic mixtures of both possible enantiomers. As there is no clear correlation between the steric demands of the dienophiles (**2** and **6** in combination with **1**) and the outcome of these cycloadditions, it is appropriate to propose that they are governed not only by the steric hindrance between the groups of the reacting molecules, but also by their electronic properties (i.e., change of stereoselectivity when oxygen dienophiles **2** are applied instead of their nitrogen analogs **6**). However, the regioselectivity of all these cycloadditions was complete, in all cases furnishing only products **3**, where the group formerly bound at position 3 in the starting 2*H*-pyran-2-ones **1** is in the product adjacent to the group stemming from the dienophiles **2** or **6**, meaning that exclusively products **3** and no **3'** are formed (see Figure 2).

The rigid 7-oxabicyclo[2.2.2]octene skeleton in compounds **3** leads to structural variations only due to rotations of side arms or to *exo/endo* orientation of substituents at position 8 as can be seen from the superposition of molecular structures (Figure 11a). At position 6, acetyl substituents incline in respect to the 7-oxabicyclo[2.2.2]octene skeleton with torsion angle Φ_1 (see Figure 11b) in the range $-179.14(15)^\circ$ (for *endo*-**3a**) and $-137.4(2)^\circ$ (for *endo*-**3e**), while benzoyl substituents in *endo*-**3d** and *exo*-**3f** incline by $138.6(3)^\circ$ and $138.9(2)^\circ$, respectively (Figure 11a). Inclination of amide group at position 4 shows much smaller differences with torsion angle Φ_2 being in the range $65.0(4)$ – $67.3(4)^\circ$ for all structures except for *exo*-**3f** where torsion angle is much larger ($172.01(17)^\circ$).

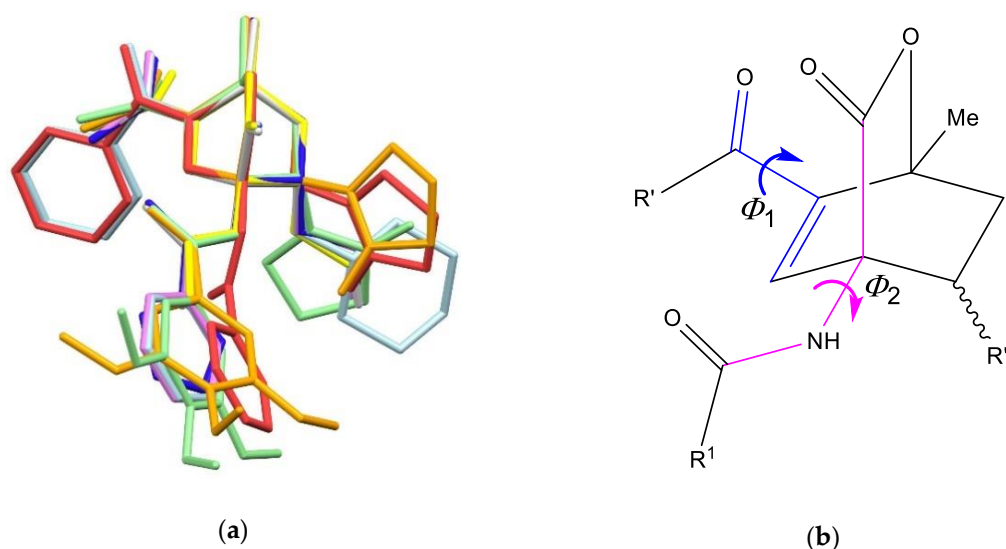


Figure 11. (a) Superposition of compounds **3**. Hydrogen atoms and disorder in *endo*-**3b** have been omitted for clarity. Color code: *endo*-**3a** (violet), *endo*-**3b** molecule A (yellow), *endo*-**3b** molecule B (light grey), *endo*-**3c** (blue), *endo*-**3d** (light blue), *endo*-**3e** (light green), *exo*-**3e** (orange), *exo*-**3f** (red); (b) torsion angles for substituents at the positions 6 and 4.

In all compounds **3**, amide NH is the only classical hydrogen bond donor and is involved in intermolecular hydrogen bonding except in compound *exo-3e*, which forms intramolecular interaction with the 2-oxopyrrolidin-1-yl substituent. When participating in intermolecular interactions diverse patterns can be expected for the amide group. For example, chains could be formed between amide units acting both as hydrogen bond donors and acceptors (see Figure 12a,b). However, among the compounds investigated in this series predominates the hydrogen bond formation between amide NH group and CO₂ bridge of the adjacent 7-oxabicyclo[2.2.2]octene molecule as observed in five out of seven cases (*endo-3a*, *endo-3b*, *endo-3c*, *endo-3d* and *exo-3f*). In most cases, centrosymmetric hydrogen-bonded dimers are formed (Figure 12c), while in *endo-3b* a centrosymmetric hydrogen-bonded tetramer is formed with a combination of the interaction between amide NH group and CO₂ bridge of the adjacent molecule and the interaction of the amide NH group with the amide carbonyl group. Such interactions in *endo-3b* are most probably possible due to the presence of two crystallographically independent molecules and/or due to the presence of sterically less demanding acetyl amino group (in comparison with benzoylamino) at position 4. On the other hand, two different patterns were found in **3e** (Figure 12d,e), in *exo-3e*, NH group is involved in intramolecular interaction with the 2-oxopyrrolidin-1-yl substituent. Such intramolecular interaction could be expected in all 2-oxopyrrolidin-1-yl-containing compounds **3** (*endo-3e-6a*, *exo-3e*, *exo-3f*) since carbonyl group can be positioned suitably for the interaction with the NH group due to the free rotation of the C–N_{pyrrolidone} bond. However, this is not the case in *endo-3e-6a* and also not in the case of *exo-3f* even though the 2-oxopyrrolidin-1-yl substituent is also in *exo* position as is in *exo-3e*. While in *exo-3e*, NH group forms intramolecular interaction with the 2-oxopyrrolidin-1-yl substituent, the situation is different in *endo-3e-6a* where NH group forms intermolecular interactions with the 2-oxopyrrolidin-1-yl substituent of the adjacent molecule. These findings imply that the *exo/endo* orientation of the 2-oxopyrrolidin-1-yl substituent is not the governing factor for the formation of hydrogen bonding with the NH group. It is worth noting that the carbonyl oxygen atom of CO₂ bridge is not involved as a hydrogen bond acceptor only in *exo-3e*, whereas in all of the other structures it is involved either in NH···O or CH···O interactions. Another interesting peculiarity of structures **3** is that ring oxygen atom of the CO₂ bridge is a hydrogen bond acceptor only in the structure of *endo-3d*.

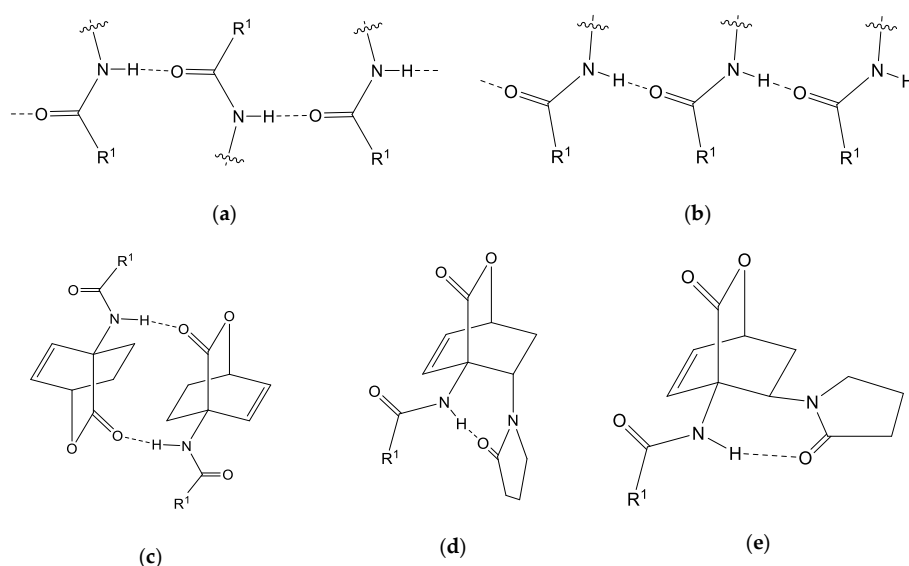


Figure 12. Possible hydrogen-bonded motifs formed by amide NH group. (a,b) chain formation through the amide groups as hydrogen bond donors and acceptors; (c) centrosymmetric hydrogen-bonded dimers with NH and CO₂ groups as hydrogen bond donor and acceptor, respectively; (d) possible intramolecular hydrogen bonding with 2-oxopyrrolidin-1-yl in *endo* position; (e) possible intramolecular hydrogen bonding with 2-oxopyrrolidin-1-yl in *exo* position.

Complete regioselectivity of the first cycloaddition step is also reflected in the formation of **4a** as the only regioisomer, again of the type having the group stemming from the dienophile **2**, and the group being in the starting 2*H*-pyran-2-one **1f** at the position 3, in 1,2-position. Therefore, cyclohexadiene product obtained was only of the type **4** (and no **4'** was detected, see Figure 1). Understandably, **4a** was formed as a racemic mixture of both possible enantiomers. Amide NH in **4a** is the only classical hydrogen bond donor and enables, in combination with centrosymmetric C–H···O interactions, the formation of hydrogen bonded layers.

5. Conclusions

We have carried out a detailed structural elucidation of cycloadducts formed between 2*H*-pyran-2-one derivatives **1** and various vinyl-moiety-containing dienophiles (ethyl vinyl ether, cyclohexyl vinyl ether and 1-vinyl-2-pyrrolidone) with oxabicyclo[2.2.2]octene skeleton (products of the type **3**) obtained only under high pressure. In all cases where oxygen-based dienophiles **2** were used (ethyl vinyl ether and cyclohexyl vinyl ether), the only stereoisomer of the products **3** obtained was of the *endo* type; however, with the nitrogen-based dienophile (1-vinyl-2-pyrrolidone) in one case (i.e., formation of **3f**) only *exo* stereoisomer was obtained, whereas in the other cases (i.e., formation of **3e**) a mixture of both *endo* and *exo* stereoisomers was produced. All of the products **3** were obtained as racemic mixtures of both possible enantiomers. However, the regioselectivity of all these cycloadditions was complete, in all cases furnishing only products **3**, where the group formerly bound at position 3 in the starting 2*H*-pyran-2-ones **1** is in the product adjacent to the group stemming from the dienophiles **2** or **6**, meaning that exclusively products **3** and no **3'** are formed.

In all 7-oxabicyclo[2.2.2]octene compounds **3**, amide NH is the only classical hydrogen bond donor and is involved in intermolecular hydrogen bonding except in compound *exo*-**3e** where intramolecular interaction is formed. The predominant motif is the intermolecular hydrogen bonding between amide NH group and CO₂ bridge of the adjacent 7-oxabicyclo[2.2.2]octene molecule as observed in five out of seven cases (*endo*-**3a**, *endo*-**3b**, *endo*-**3c**, *endo*-**3d** and *exo*-**3f**) with the domination of centrosymmetric hydrogen-bonded dimers. Diverse supramolecular patterns were observed due to rich variety of C–H···O and C–H···π interactions while no significant π···π interactions were found.

Finally, complete regioselectivity of the first cycloaddition step is also reflected in the formation of **4a** as the only regioisomer (albeit as a racemic mixture of both enantiomers). This compound represents a very rare case of a cyclohexadiene system stable at room temperature, even though it contains groups that are prone to elimination (here a molecule of ethanol could be eliminated), which would provide a benzene derivative, thus reaching aromatic stabilization. Additionally, in this case, supramolecular aggregation has been achieved through N–H···O and C–H···O interactions.

Supplementary Materials: The following are available online at <http://www.mdpi.com/2073-8994/12/10/1714/s1>, cif-files with single-crystal XRD structures of **3a–f** and **4a**.

Author Contributions: Conceptualization, K.K., M.K., F.P.; methodology, K.K., M.K., F.P.; syntheses, A.J. and K.K.; formal analysis, A.J., K.K.; X-ray diffraction, F.P.; writing—original draft preparation, K.K. and F.P.; writing—review and editing, K.K., F.P.; visualization, K.K., F.P.; funding acquisition, M.K., F.P. All authors have read and agreed to the published version of the manuscript.

Funding: This research was funded by the Ministry of Education, Science and Sport of the Republic of Slovenia and the Slovenian Research Agency, grant numbers P1-0230-0103 and P1-0230-0175.

Conflicts of Interest: The authors declare no conflict of interest.

References

1. Dyan, O.T.; Borodin, G.I.; Zaikin, P.A. The Diels–Alder reaction for the synthesis of polycyclic aromatic compounds. *Eur. J. Org. Chem.* **2019**, 7271–7306. [[CrossRef](#)]
2. Mancini, P.M.E.; Ormachea, C.M.; Kneeteman, M.N. Polar Diels–Alder reactions under microwave irradiation employing different heterocyclic compounds as electrophiles. *Mini-Rev. Org. Chem.* **2019**, *16*, 527–543. [[CrossRef](#)]

3. Harada, S.; Nishida, A. Catalytic and enantioselective Diels–Alder reactions of siloxydienes. *Asian J. Org. Chem.* **2019**, *8*, 732–745. [[CrossRef](#)]
4. Dalpozzo, R.; Bartoli, G.; Bencivenni, G. Asymmetric organocatalytic reactions of α,β -unsaturated cyclic ketones. *Symmetry* **2011**, *3*, 84–125. [[CrossRef](#)]
5. Pietrusiewicz, K.M.; Koprowski, M.; Drzazga, Z.; Parcheta, R.; Łastawiecka, E.; Demchuk, O.M.; Justyniak, I. Efficient oxidative resolution of 1-phenylphosphol-2-ene and Diels–Alder synthesis of enantiopure bicyclic and tricyclic P-stereogenic C-P heterocycles. *Symmetry* **2020**, *12*, 346. [[CrossRef](#)]
6. Rádai, Z.; Bagi, P.; Czugler, M.; Karaghiosoff, K.; Keglevich, G. Optical resolution of dimethyl α -hydroxy-arylmethylphosphonates via diastereomer complex formation using calcium hydrogen *O,O'*-dibenzoyl-(2*R*,3*R*)-tartrate; X-ray analysis of the complexes and products. *Symmetry* **2020**, *12*, 758. [[CrossRef](#)]
7. Soai, K.; Kawasaki, T.; Matsumoto, A. Role of asymmetric autocatalysis in the elucidation of origins of homochirality of organic compounds. *Symmetry* **2019**, *11*, 694. [[CrossRef](#)]
8. Hoffmann, R.; Woodward, R.B. The conservation of orbital symmetry. *Acc. Chem. Res.* **1968**, *1*, 17–22. [[CrossRef](#)]
9. Woodward, R.B.; Hoffmann, R. Selection rules for concerted cycloaddition reactions. *J. Am. Chem. Soc.* **1965**, *87*, 2046–2048. [[CrossRef](#)]
10. Sauer, J.; Sustmann, R. Mechanistic aspects of Diels–Alder reactions: A critical survey. *Angew. Chem. Int. Ed.* **1980**, *19*, 779–807. [[CrossRef](#)]
11. Uemura, N.; Toyoda, S.; Shimizu, W.; Yoshida, Y.; Mino, T.; Sakamoto, M. Absolute asymmetric synthesis involving chiral symmetry breaking in Diels–Alder reaction. *Symmetry* **2020**, *12*, 910. [[CrossRef](#)]
12. Kitagawa, D.; Bardeen, C.J.; Kobatake, S. Symmetry breaking and photomechanical behavior of photochromic organic crystals. *Symmetry* **2020**, *12*, 1478. [[CrossRef](#)]
13. Ram, V.J.; Srivastava, P. Pyran-2-ones as a versatile synthon for the synthesis of diverse arenes and heteroarenes. *Curr. Org. Chem.* **2001**, *5*, 571–599. [[CrossRef](#)]
14. Afarinkia, K.; Vinader, V.; Nelson, T.D.; Posner, G.H. Diels–Alder cycloadditions of 2-pyrones and 2-pyridones. *Tetrahedron* **1992**, *48*, 9111–9171. [[CrossRef](#)]
15. Štefane, B.; Perdih, A.; Pevec, A.; Šolmajer, T.; Kočevár, M. The participation of 2*H*-pyran-2-ones in [4 + 2] cycloadditions: An experimental and computational study. *Eur. J. Org. Chem.* **2010**, 5870–5883. [[CrossRef](#)]
16. Kranjc, K.; Kočevár, M. Ethyl vinyl ether as a synthetic equivalent of acetylene in a DABCO-catalyzed microwave-assisted Diels–Alder–elimination reaction sequence starting from 2*H*-pyran-2-ones. *Synlett* **2008**, 2613–2616. [[CrossRef](#)]
17. Juranovič, A.; Kranjc, K.; Perdih, F.; Polanc, S.; Kočevár, M. Comparison of the reaction pathways and intermediate products of a microwave-assisted and high-pressure-promoted cycloaddition of vinyl-moiety-containing dienophiles on 2*H*-pyran-2-ones. *Tetrahedron* **2011**, *67*, 3490–3500. [[CrossRef](#)]
18. Cole, C.J.F.; Fuentes, L.; Snyder, S.A. Asymmetric pyrone Diels–Alder reactions enabled by dienamine catalysis. *Chem. Sci.* **2020**, *11*, 2175–2180. [[CrossRef](#)]
19. Geist, E.; Berneaud-Kötz, H.; Baikstis, T.; Dräger, G.; Kirschning, A. Toward chromanes by de novo construction of the benzene ring. *Org. Lett.* **2019**, *21*, 8930–8933. [[CrossRef](#)]
20. Grant, P.S.; Brimble, M.A.; Furkert, D.P. Synthesis of the bicyclic lactone core of leonuketol, enabled by a telescoped Diels–Alder reaction sequence. *Chem. Asian J.* **2019**, *14*, 1128–1135. [[CrossRef](#)] [[PubMed](#)]
21. Kondratov, I.S.; Tolmachova, N.A.; Dolovanyuk, V.G.; Gerus, I.I.; Daniliuc, C.-G.; Haufe, G. Synthesis of trifluoromethyl-containing polysubstituted aromatic compounds by Diels–Alder reaction of ethyl 3-benzamido-2-oxo-6-(trifluoromethyl)-2*H*-pyran-5-carboxylate. *Eur. J. Org. Chem.* **2015**, 2482–2491. [[CrossRef](#)]
22. Kondratov, I.S.; Tolmachova, N.A.; Dolovanyuk, V.G.; Gerus, I.I.; Bergander, K.; Daniliuc, C.-G.; Haufe, G. Diels–Alder reaction of ethyl 3-benzamido-2-oxo-6-(trifluoromethyl)-2*H*-pyran-5-carboxylate with alkoxyalkenes as an effective approach to trifluoromethyl-containing 3-aminobenzoic acid derivatives. *Eur. J. Org. Chem.* **2014**, 2443–2450. [[CrossRef](#)]
23. Burch, P.; Binaghi, M.; Scherer, M.; Wentzel, C.; Bossert, D.; Eberhardt, L.; Neuburger, M.; Scheiffele, P.; Gademann, K. Total synthesis of gelsemiol. *Chem. Eur. J.* **2013**, *19*, 2589–2591. [[CrossRef](#)] [[PubMed](#)]
24. Bartelson, K.J.; Singh, R.P.; Foxman, B.M.; Deng, L. Catalytic asymmetric [4 + 2] additions with aliphatic nitroalkenes. *Chem. Sci.* **2011**, *2*, 1940–1944. [[CrossRef](#)]

25. Afarinkia, K.; Abdullahi, M.H.; Scowen, I.J. A new, general method for the synthesis of carbasugar-sugar pseudodisaccharides. *Org. Lett.* **2009**, *11*, 5182–5184. [[CrossRef](#)]
26. Wang, Y.; Li, H.; Wang, Y.-Q.; Liu, Y.; Foxman, B.M.; Deng, L. Asymmetric Diels–Alder reactions of 2-pyrone with a bifunctional organic catalyst. *J. Am. Chem. Soc.* **2007**, *129*, 6364–6365. [[CrossRef](#)]
27. Shimo, T.; Yasutake, M.; Shinmyozu, T.; Somekawa, K. Crystal structure of methyl endo-8-cyano-exo-8-methyl-3-oxo-2-oxabicyclo[2.2.2]oct-5-ene-6-carboxylate. *Anal. Sci.* **2003**, *19*, 471–472. [[CrossRef](#)]
28. Zhang, H.; Appels, D.C.; Hockless, D.C.R.; Mander, L.N. A new approach to the total synthesis of the unusual diterpenoid tropone, harringtonolide. *Tetrahedron Lett.* **1998**, *39*, 6577–6580. [[CrossRef](#)]
29. Hren, J.; Polanc, S.; Kočevar, M. The synthesis and transformations of fused bicyclo[2.2.2]octenes. *Arkivoc* **2008**, *i*, 209–231. [[CrossRef](#)]
30. Kranjc, K.; Kočevar, M. Green chemistry starting from 2H-pyran-2-one derivatives. *Curr. Green Chem.* **2014**, *1*, 202–215. [[CrossRef](#)]
31. Kranjc, K.; Kočevar, M. Regio- and stereoselective syntheses and cycloadditions of substituted 2H-pyran-2-ones and their fused derivatives. *Arkivoc* **2013**, *i*, 333–363. [[CrossRef](#)]
32. Kranjc, K.; Polanc, S.; Kočevar, M. Diels–Alder reactions of fused pyran-2-ones with maleimides: Efficient syntheses of benz[e]isoindoles and related systems. *Org. Lett.* **2003**, *5*, 2833–2836. [[CrossRef](#)]
33. Kranjc, K.; Perdih, F.; Kočevar, M. Effect of ring size on the *exo/endo* selectivity of a thermal double cycloaddition of fused pyran-2-ones. *J. Org. Chem.* **2009**, *74*, 6303–6306. [[CrossRef](#)] [[PubMed](#)]
34. Krivec, M.; Gazvoda, M.; Kranjc, K.; Polanc, S.; Kočevar, M. A way to avoid using precious metals: The application of high-surface activated carbon for the synthesis of isoindoles via the Diels–Alder reaction of 2H-pyran-2-ones. *J. Org. Chem.* **2012**, *77*, 2857–2864. [[CrossRef](#)] [[PubMed](#)]
35. Gladysz, J.A.; Lee, S.J.; Tomasello, J.A.V.; Yu, Y.S. High-pressure cycloadditions of pyrones: Synthesis of highly functionalized six-membered rings by inhibition of carbon dioxide loss. *J. Org. Chem.* **1977**, *42*, 4171–4172. [[CrossRef](#)]
36. Klärner, F.-G.; Breitkopf, V. The effect of pressure on retro Diels–Alder reactions. *Eur. J. Org. Chem.* **1999**, 2757–2762. [[CrossRef](#)]
37. Uroos, M.; Pitt, P.; Harwood, L.M.; Lewis, W.; Blake, A.J.; Hayes, C.J. Total synthesis of (–)-aritasone via the ultra-high pressure hetero-Diels–Alder dimerisation of (–)-pinocarvone. *Org. Biomol. Chem.* **2017**, *15*, 8523–8528. [[CrossRef](#)] [[PubMed](#)]
38. Yadav, V.K.; Prasad, D.L.V.K.; Yadav, A.; Yadav, K. On the solvent- and temperature-driven stereoselectivity of the Diels–Alder cycloaddition reactions of furan with maleic anhydride and maleimide. *J. Phys. Org. Chem.* **2020**, e4131. [[CrossRef](#)]
39. Tsypysheva, I.P.; Borisevich, S.S.; Lobov, A.N.; Kovalskaya, A.V.; Shamukaev, V.V.; Safiullin, R.L.; Khursan, S.L. Inversion of diastereoselectivity under high pressure conditions: Diels–Alder reactions of 12-*N*-substituted derivatives of (–)-cytisine with *N*-phenylmaleimide. *Tetrahedron Asymmetry* **2015**, *26*, 732–737. [[CrossRef](#)]
40. Webb, J.N.; Marsden, P.S.; Raw, A.S. Rhodium(III)-catalyzed C–H activation/annulation with vinyl esters as an acetylene equivalent. *Org. Lett.* **2014**, *16*, 4718. [[CrossRef](#)]
41. Toure, M.; Jaime-Figueroa, S.; Burslem, G.M.; Crews, C.M. Expedient synthesis of isoquinolones and isocoumarins with a vinyl borane as an acetylene equivalent. *Eur. J. Org. Chem.* **2016**, 4171–4175. [[CrossRef](#)]
42. Desiraju, G.R. Crystal Engineering: From Molecule to Crystal. *J. Am. Chem. Soc.* **2013**, *135*, 9952–9967. [[CrossRef](#)] [[PubMed](#)]
43. Gavezzotti, A. Pillars of crystal engineering: Crystal energies and symmetry operators. *CrystEngComm* **2018**, *20*, 2511–2518. [[CrossRef](#)]
44. Lengauer, H.; Makuc, D.; Šterk, D.; Perdih, F.; Pichler, A.; Trdan Lušin, T.; Plavec, J.; Časar, Z. Co-crystals, salts or mixtures of both? The case of tenofovir alafenamide fumarates. *Pharmaceutics* **2020**, *12*, 342. [[CrossRef](#)] [[PubMed](#)]
45. Bolotin, D.S.; Il'in, M.V.; Suslonov, V.V.; Novikov, A.S. Symmetrical noncovalent interactions Br⋯Br observed in crystal structure of exotic primary peroxide. *Symmetry* **2020**, *12*, 637. [[CrossRef](#)]
46. Otwinowski, Z.; Minor, W. Processing of X-ray diffraction data collected in oscillation mode. *Methods Enzymol.* **1997**, *276*, 307–326.
47. Sheldrick, G.M. A short history of SHELX. *Acta Cryst.* **2008**, *64*, 112–122. [[CrossRef](#)]
48. Kappe, C.O. My twenty years in microwave chemistry: From kitchen ovens to microwaves that aren't microwaves. *Chem. Rec.* **2019**, *19*, 15–39. [[CrossRef](#)]

49. Sarotti, A.M.; Pisano, P.L.; Pellegrinet, S.C. A facile microwave-assisted Diels–Alder reaction of vinylboronates. *Org. Biomol. Chem.* **2010**, *8*, 5069–5073. [[CrossRef](#)]
50. Tajti, Á.; Szatmári, E.; Perdih, F.; Keglevich, G.; Bálint, E. Microwave-assisted Kabachnik–Fields reaction with amino alcohols as the amine component. *Molecules* **2019**, *24*, 1640. [[CrossRef](#)]
51. Bernstein, J.; Davis, R.E.; Shimoni, L.; Chang, N.-L. Patterns in Hydrogen Bonding: Functionality and Graph Set Analysis in Crystals. *Angew. Chem. Int. Ed. Engl.* **1995**, *34*, 1555–1573. [[CrossRef](#)]
52. Afarinkia, K.; Abdullahi, M.H.; Scrowen, I.J. A synthesis of carbasugar–sugar pseudodisaccharides via a cycloaddition–cycloreversion reaction of 2*H*-pyran-2-ones. *Org. Lett.* **2010**, *12*, 5564–5566. [[CrossRef](#)]
53. Drljaca, A.; Hubbard, C.D.; van Eldik, R.; Asano, T.; Basilevsky, M.V.; le Noble, W.J. Activation and reaction volumes in solution. 3. *Chem. Rev.* **1998**, *98*, 2167–2289. [[CrossRef](#)] [[PubMed](#)]
54. Van Eldik, R.; Asano, T.; le Noble, W.J. Activation and reaction volumes in solution. 2. *Chem. Rev.* **1989**, *89*, 549–688. [[CrossRef](#)]

Publisher’s Note: MDPI stays neutral with regard to jurisdictional claims in published maps and institutional affiliations.



© 2020 by the authors. Licensee MDPI, Basel, Switzerland. This article is an open access article distributed under the terms and conditions of the Creative Commons Attribution (CC BY) license (<http://creativecommons.org/licenses/by/4.0/>).